ADVANCED OPTICAL MATERIALS

Supporting Information

for *Advanced Optical Materials,* DOI: 10.1002/adom.201801746

Asymmetric Diarylethenes with Oxidized 2-Alkylbenzothiophen-3-yl Units: Chemistry, Fluorescence, and Photoswitching

Kakishi Uno, Mariano L. Bossi, Timo Konen, Vladimir N. Belov,* Masahiro Irie,* and Stefan W. Hell*

Supporting Information

Asymmetric diarylethenes with oxidized 2-alkylbenzothiophen-3-yl units: chemistry, fluorescence and photoswitching

Kakishi Uno[#], Mariano L. Bossi[#],* Timo Konen, Vladimir N. Belov,* Masahiro Irie,* and Stefan W. Hell

[#] equal contributions

Asymmetric diarylethenes with 2-alkyl-1-benzothiophen-1,1-dioxide-3-yl units: chemistry, fluorescence and photoswitching

Kakishi Uno[#], Mariano L. Bossi[#], Timo Konen, Vladimir N. Belov, Masahiro Irie[†], and Stefan W. Hell

Department of NanoBiophotonics, Max Planck Institute for Biophysical Chemistry, Am Fassberg 11, 37077 Göttingen, Germany

[†]Research Center for Smart Molecules, Department of Chemistry, Rikkyo University, Nishi-Ikebukuro 3-34-1, Toshimaku, Tokyo, Japan

# equal contributions

Abbreviations

The following abbreviations are used in the text of the *Supplementary Information*:

acetonitrile (MeCN), anti-parallel (ap), aqueous (aq.), argon (Ar), bis(pinacolato)diboron $(Bpin)_2$, bovine serum albumin (BSA), catalysis (cat.), closed form (CF), diarylethene (DAE), dichloromethane (DCM), dimethyl sulfoxide (DMSO), electrospray ionization (ESI), ethyl acetate (EtOAc), fluorescent diarylethene (fDAE), high performance liquid chromatography (HPLC), high resolution mass spectrometry (HR-MS), magnesium sulfate ($MgSO_4$), methanol (MeOH), *N*-hydroxysuccinimide (NHS), *N,N*-dimethylformamide (DMF), nitrogen (N_2), nuclear magnetic resonance (NMR), open form (OF), parallel (p), phosphate buffer saline (PBS), photo stationary state (PSS), potassium acetate (KOAc), reverse phase (RP), room temperature (r.t.), saturated (sat.), tetrahydrofurane (THF), thin layer chromatography (TLC), tricyclohexylphosphine (PCy_3), triethylamine (TEA), trifluoroacetic acid (TFA), ultraviolet (UV), visible (Vis.), volume ratio of two solvents (v/v).

High-performance liquid chromatography separations

Preparative HPLC was performed on an Interchim puriFlash 4250 2X preparative HPLC/Flash hybrid system (Article No. 1I5140, Interchim) with 2 mL or 5 mL injection loops, a 200-600 nm UV-Vis detector and an integrated ELSD detector (Article No. 1A3640, Interchim). Preparative column: Interchim Uptisphere Strategy C18-HQ, 10 µm, 250×21.2 mm (Article No. US10C18HQ-250/212, Interchim), typical flow rate: 20 mL/min, unless specified otherwise. Analytical TLC was performed on Merck Millipore ready-to-use plates with silica gel 60 (F254). Preparative TLC was performed on precoated thin-layer plates with silica gel for high performance TLC (HPTLC Silica gel 60 F254 10×10 cm, layer thickness 150-200 µm, with concentrating zone 10 x 2.5 cm), purchased from Merck Millipore. Flash chromatography was performed on Biotage Isolera flash purification system using the type of cartridge and solvent gradient indicated. Analytical HPLC was performed on a Shimadzu Prominence system with a photodiode array detector (SPD-M20A), with a 20 µL injection loop, and a 150 × 4 mm column (Knauer, Eurospher II 100-10 C18A with precolumn, Vertex Plus Column), at a flowrate of 2 mL/min with water/MeCN gradient, and both solvents containing 0.1% of TFA.

Photochemical characterizations

1. **Photo-switching setup**

Irradiation experiments were performed in a home-made setup, containing two high power light emitting diodes LED (Thorlabs, M365L2 and M470L3) as irradiation sources, and a fiber-coupled diode array spectrometer (Ocean Optics, Flame-S UV-Vis configuration). For absorption measurements, a fiber-coupled halogen/deuterium light source (Ocean Optics, DH-2000-BAL) was used at 180 degrees. The sample was placed in a quartz fluorescent cuvette (Hellma Analytics, 119F-10-40), in a Peltier-based temperature-controlled cuvette holder, with four optical ports and magnetic stirring (Quantum Northwestern, Luma 40). A set of lenses and circular apertures were used to ensure the irradiation beams are approximately collimated and with a diameter of around 6 mm at the sample. The collimation of the optical fibers at the sample holder was achieved by dedicated achromatic lenses (Ocean Optics, 74-UV). A schematic representation of the setup is provided in Figure S1. The system is controlled from a PC with homemade routines written in Matlab. A data acquisition system (National Instruments, myDAQ) is used to control the shutter of the lamp, and the drivers of the LEDs, via TTL signals (digital outputs).

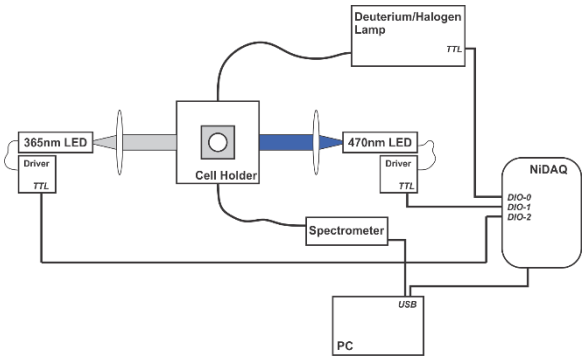

Figure S1. Schematic representation of the setup.

In a typical experiment, the programs open the shutter of the lamp and record an absorption (and emission, if desired) spectrum, then switch-on one of the LEDs for a determined irradiation (t_{IRR}), switch off the irradiation LED and record an absorption spectrum again. To record the absorption, the shutter of the halogen/deuterium source is temporarily open, and for the emission spectrum, one of the LEDs is used as the excitation source for a short period of time, typically 1-4 µs, much lower than any irradiation time (typically from 100 ms to several seconds). Previous to any irradiation sequence, control experiments are run to ensure that the interrogation of the system does not change its state (i.e. no isomerization in any direction is observable under the selected integration time of the absorption and emission spectrum). The software allows for almost any desired sequence of steps, but the two main experiments are (1) the switching kinetics, for the determination of the isomerization quantum yields, and (2) a cycling experiment. In the first one, the absorption (and emission) is determined at small irradiation steps of the same LED, to record a single reaction conversion transient, OF→CF or CF→OF (see for example Figure 2A and 2B in the main text). In the second, two irradiation steps with alternating LED (UV/VIS) are repeated, typically with irradiation times t_{UV} and t_{VIS}, each one long enough to ensure conversion to the corresponding photo-stationary state, PSS-UV and PSS-VIS, respectively (see for example Figure 2C-D in the main text). Absorption (and emission) was probed after each step. Because all DAEs studied are bistable, the irradiation sources were switched off during the interrogation of the system (absorption measurements) except for the excitation of fluorescence, and the spectrometer lamp was switched off during irradiations. The intensity of the irradiation light was calibrated using chemical actinometers; [1] for UV light (365 nm), azobenzene in MeOH was used,[2] and for visible light (470nm), we used the ring-opening reaction of the fulgide Aberchrome 670 in toluene.[3]

2. Absorption and emission of DAEs

Absorption spectra were recorded in a Cary5000 UV-Vis-NIR spectrophotometer (Agilent Technologies). Fluorescence emission spectra were recorded in a Cary Eclipse Fluorescence Spectrophotometer (Agilent Technologies), and fluorescence lifetimes in a FluoTime 300 Fluorescence Lifetime Spectrophotometer (PicoQuant). Quartz cuvettes with 1 cm path and four clear windows (Hellma Analytics) were used in all experiments. In Figure S2, the absorption and emission of all studied compounds in MeOH are presented.

The poor photo-stability of compound **1**-CN,N is evidenced by the presence of a photoproduct, distorting the absorption spectrum of the CF, appearing as a shoulder at 360 nm. The amount of this byproduct is not negligible for this compound, even in the first irradiation to the PSS-365nm. For all the other compounds, the amount of byproducts can be neglected, and become observable only after several irradiation cycles. A determining factor for this distinct behavior of compound 3 is probable the high ratio between the absorption coefficients of the CF and the OF at the irradiation wavelength ($\varepsilon_{CF}^{365nm}/\varepsilon_{OF}^{3656nm}$) of 23, compared with the rest of the compounds prepared, presenting ratios in the range 0.6 – 3.3. In addition, the absorption coefficient of **1**-CN,N -CF at the irradiation wavelength is also higher (2-fold to 5-fold) than any other CF.

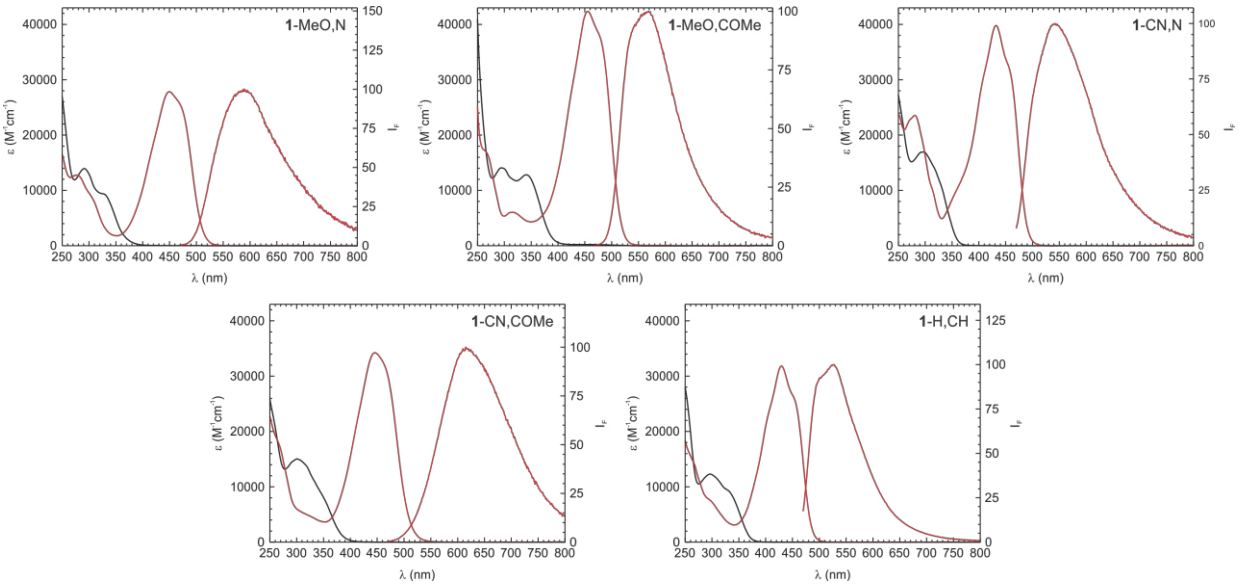

Figure S2. Absorption spectra of the OF (black lines), CF (red lines) for the five DAEs prepared in this work. The absorption of the CF was calculated from the HPLC traces and the absorption spectra of the peaks in the photo-stationary state under irradiation with 365 nm light, using the measured conversion ($\alpha_{PSS\text{-}365nm}$). The emission spectra of the CF (red lines, right axis) was measured at low conversions, when the absorption of the CF at the maximum is below 0.05.

3. Determination of the conversion in the PSS and isomerization quantum yields

Irradiated solution (~10 µM in MeOH) in the PSS were directly injected into the analytical HPLC (see section 2) and separated using solvent gradients of 20 – 75 % MeCN (TFA 0.1 %) / 80 – 25 % water (TFA 0.1 %), with the exception of compound **1**-H,H, that was separated using gradients of 40 – 50 % MeCN (TFA 0.1 %) / 60 – 50 % water (TFA 0.1%). Then, two methods were used to calculate the conversion ($\alpha_{PSS\text{-}365nm}$). In the first one, the chromatogram at the wavelength of the isosbestic point was integrated:

$$\alpha_{PSS}^{365nm} = \frac{Area_{CF}}{Area_{OF} + Area_{CF}}$$

In the second method, the spectra of each isomer was extracted, and normalized at the wavelength of the isosbestic point. Then, we found the best linear combination of these two spectra that matches the absorption spectrum at the PSS. The coefficients represents the proportion of each isomer in the PSS. Both methods are sensitive to errors arising from changes in the spectrum in the different solvents used for irradiation and for HPLC elution. In general similar results were obtained, but the second method is more reliable because it uses the whole spectrum, and thus a direct observation of the error is possible. As an example, the results obtained for compound **1**-MeO,COMe are presented in Figure S2.

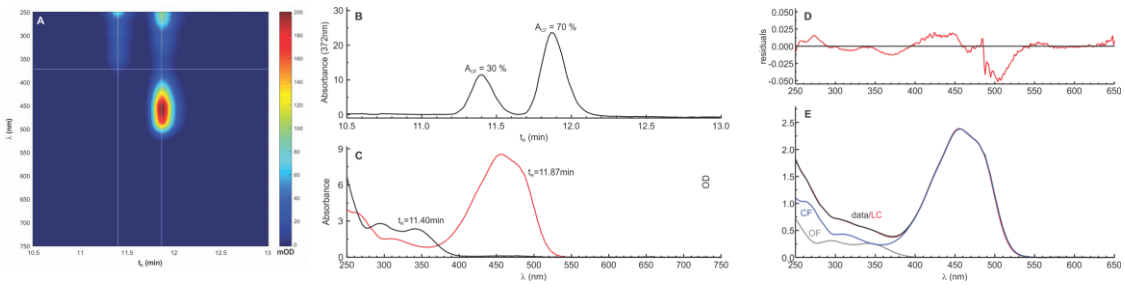

Figure S3. (A) Chromatogram (2D map) of a solution of compound **1**-MeO,COMe irradiated to the PSS-365nm. The horizontal white line correspond to the data in (B), and the vertical white lines to the spectrum in (C). (B) Intensity at the isobestic wavelength (372 nm), with the integrated area for each peak. (C) Absorption spectra at the indicated retention time, corresponding to the OF (black line) and the CF (red lines), normalized at the isobestic point. (D, E) The absorption spectrum at the PSS-365nm (data, black line), and the linear combination (LC, red line) of the spectrum of the OF (gray line) and the CF (blue line), both scaled by the resulting factors. The residuals (data-LC) are shown in the upper plot (D). Note that the spectrum of the OF and CF in (E) are those extracted from (C), but the one from the OF was corrected from the small amount of CF present due to the isomerization occurring at the diode array detector.

Isomerization quantum yields were determined from conversion curves (see, for example, Figurs 2 and S5), according to established methods. [Deniel M.H., Lavabre D., Micheau J.C. (2002)

Photokinetics under Continuous Irradiation. In: Crano J.C., Guglielmetti R.J. (eds) Organic Photochromic and Thermochromic Compounds. Topics in Applied Chemistry. Springer, Boston, MA (ISBN: 978-0-306-45883-5)] Conversion curves, such as those presented in Figure 2B and Figure S5, where fitted to monoexponential functions, in the cases were the photokinetic factor (F = {[1-10^{-A}]/A}) at the irradiation wavelength was approximated constant (e.g. in diluted solutions), or numerically integrated. In cases were high photobleaching was found (e.g. compound **1**-CN,N in MeOH and water), isomerization quantum yields were determined from initial rates at low conversions (<5%).

4. Photochemical properties in acetonitrile, methanol and water

The emission quantum yield Φ_{FI} and the conversion speed ($\varepsilon_{OF}\times\Phi_{OF\rightarrow CF}$) in MeCN and water are presented in Table S1, normalized by the value measured in MeOH. Absolute values in MeOH are presented in Table 1 on the main text.

Table S1. Comparative properties of the DAEs in different solvents, with methanol as the reference solvent.

DAE	Substitution pattern	Φ_{FI}		$\varepsilon_{OF}\times\Phi_{OF\rightarrow CF}$ [a]		$\varepsilon_{CF}\times\Phi_{CF\rightarrow OF}$ [a]	
		MeCN	H_2O	MeCN	H_2O	MeCN	H_2O
***1**-MeO,N*	D-A	0,88	0,48	1,25	0,69	1,95	0,44
***1**-MeO,COMe*	D-D	0,97	0,44	0,92	0,56	1,10	0,53
***1**-CN,N*	A-A	0,95	0,49	1,13	1,09	1,15	0,55
***1**-CN,COMe*	A-D	1,45	0,35	0,53	0,24	1,01	0,39
***1**-H,CH*	H-H	1,11	0,58	1,10	1,08	1,12	0,71

a) units: [L mol^{-1} cm^{-1}]

Fatigue resistance of compound **1**-MeO,N in the three studied solvents is given in Figure S4. Switching times were adjusted to the velocities observed in each solvent.

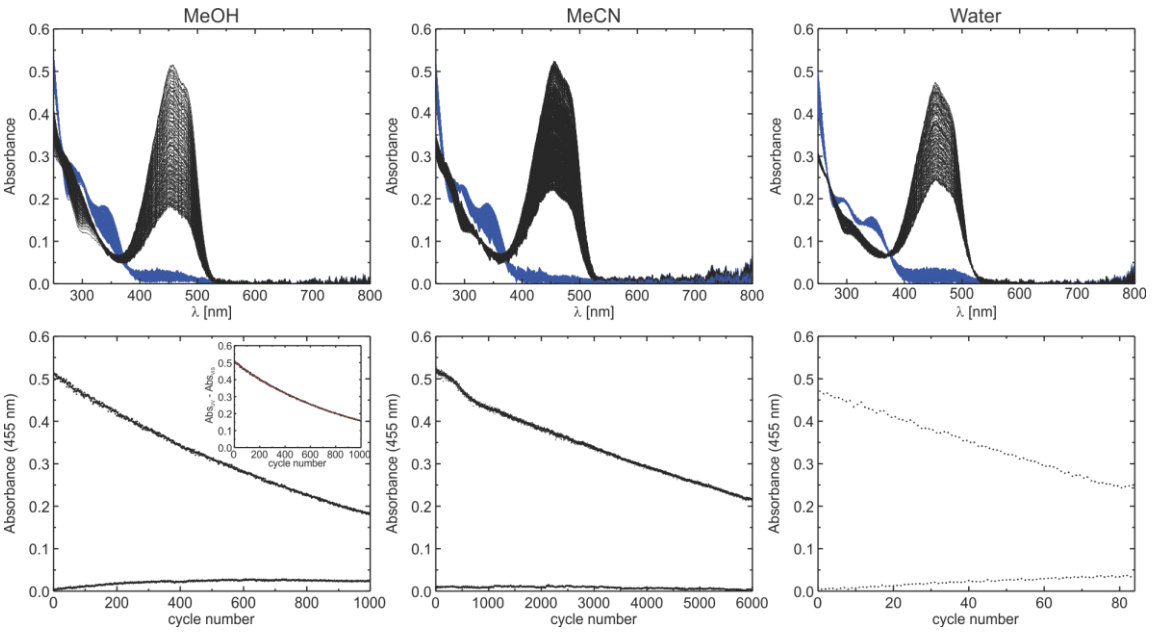

Figure S4. Photoswitching of DAE **1**-MeO,COMe in methanol, acetonitrile and water. The spectra of each 20th cycle are plotted in the upper row. Irradiation intensities: 2.3×10^{-4} einstein dm^{-3} s^{-1} (365

nm) and 3.9×10^{-4} einstein dm^{-3} s^{-1} (470 nm). In the inset, the difference in the absorption at 455 nm after each cycle ($OD_{\lambda CF}$-UV – $OD_{\lambda CF}$-VIS) is plotted *vs* the cycle number. The red line (insert on the left side of the lower row) represents an exponential fit, used to calculate $N_{½}$. If the data did not fit an exponential function (e.g., in water for this compound), $N_{½}$ was estimated manually.

5. Dependence of the fatigue resistance upon UV irradiation (switching) time, and water content of the solvent

Compound **1**-MeO,COMe was selected for this experiment because it appeared to be a promising label for biological macromolecules. We used aqueous mixtures/solutions, because water is the most relevant solvent to find imaging conditions applicable in biology-related microscopy. The results are shown in Figure S5.

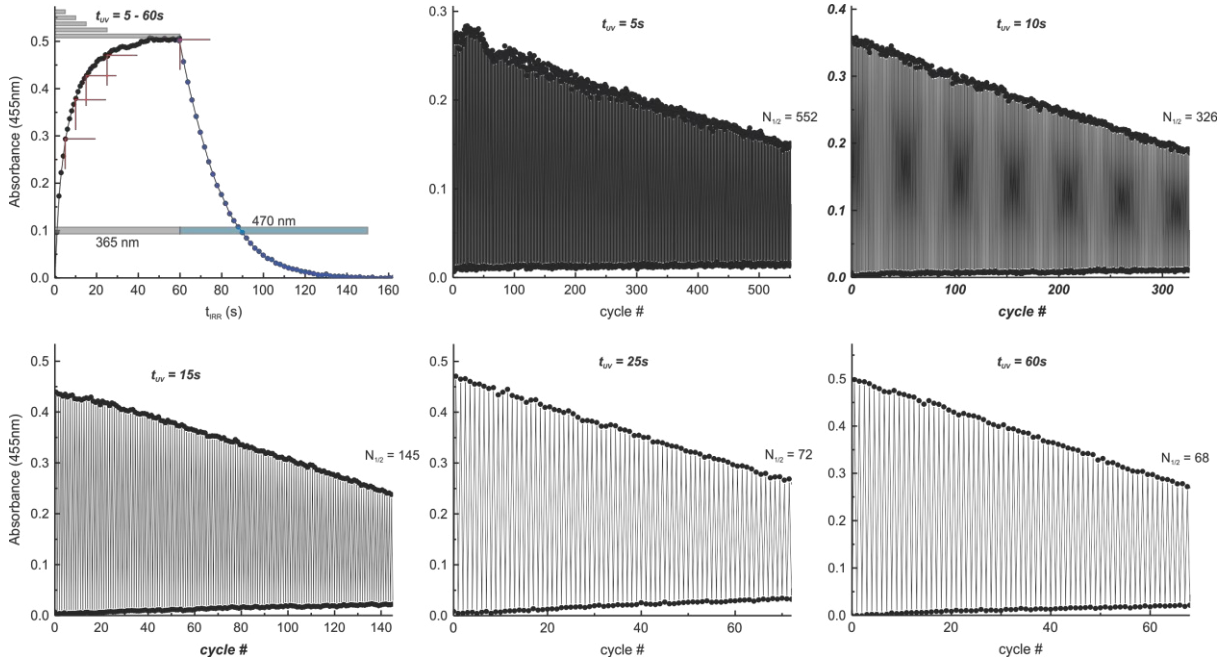

Figure S5. Dependence of the fatigue resistance of dye **1**-MeO,COMe (D-D) in aqueous solutions upon irradiation time. Irradiation with UV (365 nm) light for 5, 10, 15, 25 and 60 s. The irradiation time with visible (470 nm) light was kept constant at 90 s. Irradiation intensities: 2.3×10^{-4} einstein dm^{-3} s^{-1} (365 nm) and 3.9×10^{-4} einstein dm^{-3} s^{-1} (470 nm).

6. Protein labeling and photoswicthing

BSA was selected as a model protein to optimize the amounts of the reactive dye (NHS ester) in the labelling protocol (see refs. 4 and 8 in the main text) and to investigate the switching performance of the conjugates in aqueous solutions. The absorption spectra of the unlabeled protein and the three conjugates prepared with compound **1**-MeO,COMe, along with the values of DOL calculated by using UV-Vis spectroscopy, are presented in Figure S6C. The total amount of dye (OF+CF) was used for the

calculation of the DOL-value, assuming that the dye has the same absorption coefficients being attached to proteins (in aqueous PBS) and in solution in methanol.

The fatigue resistance of the conjugate with DOL 5.1 was investigated in PBS at a concentration of 70 µg/ml; an equivalent concentration of the dye is 5 µM (Figure S6). The results confirm that **1**-MeO,COMe retains the photochromic and fluorescent properties being bound with a protein. The $N_{½}$ value determined from the absorption is 19 cycles, while the fluorescence modulation yields 30 cycles. The difference is due to a shift of the absorption baseline which was observed (probably, due to aggregation or precipitation of the protein, after photo-bleaching of the marker). Thus, we consider the value measured by fluorescence to be more precise and relevant for microscopy experiments. A similar experiment with the conjugate having DOL = 8.1 yielded values of $N_{½}$ = 11 and 20 by absorption and emission, respectively (data not shown). Therefore, antibodies were labelled with DOLs < 5.

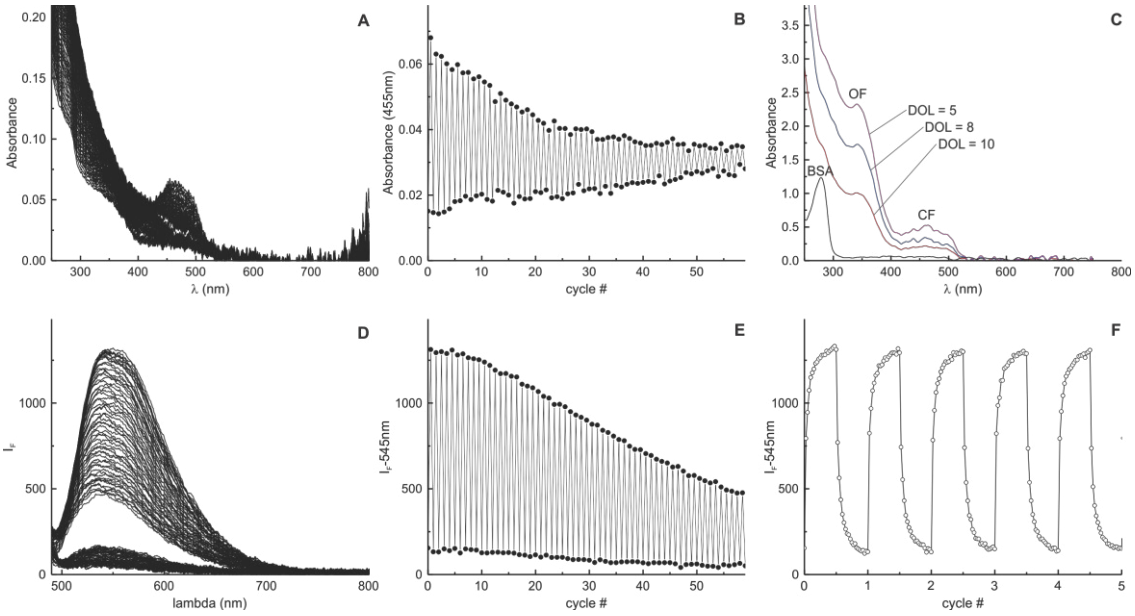

Figure S6. Photoswitching of BSA-***1****-MeO,COMe* conjugate with DOL = 5.1 in PBS (pH = 7.4). (A, D) Absorption and emission (λ_{EX} = 470 nm) after each semi-cycle (365 nm / 470 nm irradiation). (B, E) absorption and emission intensities at the corresponding maxima of the "closed" fluorescent isomer. (F) Fluorescence modulation at the emission maximum for the first five complete cycles, with 20 intermediate points for each semi-cycle. (C) Absorption spectra of the three BSA conjugates with the calculated DOL values; the bands of the "open" and "closed" isomers of the DAE unit are marked in the graph. The intensity of the irradiation light in this experiment was 2.3×10^{-4} einsteins dm^{-3} s^{-1} (365 nm) and 3.9×10^{-4} einsteins dm^{-3} s^{-1} (470 nm). A similar experiment with the conjugate having DOL = 8.1 gave values of $N_{½}$ = 11 and 20, evaluated by measuring absorption and emission intensities, respectively.

7. Immunostaining and imaging

We used a standard protocol for immunostaing fixed cells. Vero or Hela cells were grown on high glucose DMEM (Dulbecco's Modified Eagle Medium, Gibco) supplemented with glutamate and fetal bovine serum (FBS, Gibco), and plated on coverslips one day previous to the experiment. Cells were fixed by adding MeOH cooled to -20 °C for 4 min at RT, washed with PBS for 5 min and then washed two times with a blocking buffer (BSA 2 % in PBS). A primary antibody was let reacting for 1 h in blocking buffer at RT, and then washed three times with blocking buffer (5 minutes each time). Secondary antibodies labelled with a DAE were applied and let to react for 1 h in blocking buffer at RT, then washed three times with blocking buffer (5 minutes each time), and, finally, with PBS. Samples were immediately mounted on concavity microscope slides, with PBS as a mounting media, and sealed with nail polishing. Samples were imaged 1-2 hours after mounting (Figure S7), but in general were stable for at least 24 hours, when kept in a fridge.

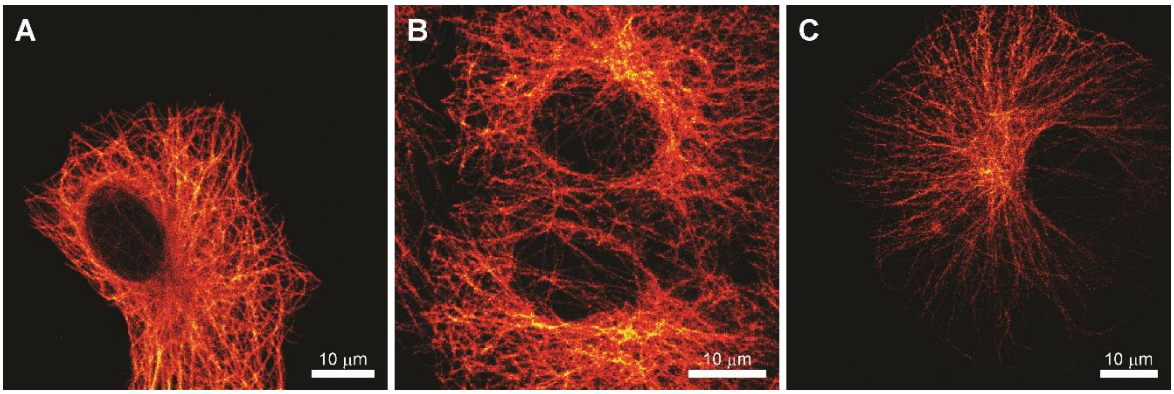

Figure S7. Confocal imaging of Vero cells immunostained with secondary antibodies labelled with (A) compound **1**-MeO,COMe (DOL 5.0), (B) compound **1**-CN,COMe (DOL 3.1), and (C) compound **1**-H,CH (DOL 3.8). A primary antibody against tubulin was used. Cells were mounted and imaged in PBS.

The photoswitching of the labeled antibodies was verified in confocal wide-field imaging. Samples were exposed first to UV light (DAPI filter-cube) for a few seconds (1-5 s), and then imaged in confocal mode. Series of ten frames were recorded. In-between series, the samples were exposed to UV light in wide-field illumination (Figure S8 – S9).

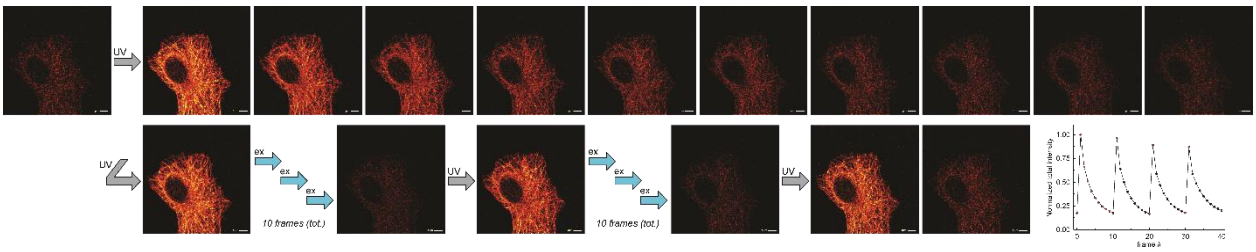

Figure S8. Confocal imaging of Vero cells immunostained with a secondary antibody labelled with compound **1**-MeO,COMe (DOL 5.0) and a primary antibody against tubulin. The sample was first exposed to UV light in wide-field illumination, to switch-on the marker (OF→CF). Then, a series of ten frames under identical conditions was recorded (top panel). The process was repeated another three times; only the first and the last images of these series are shown (lower panel). Initially, the sample was switched a few times, to focus and optimize imaging conditions.

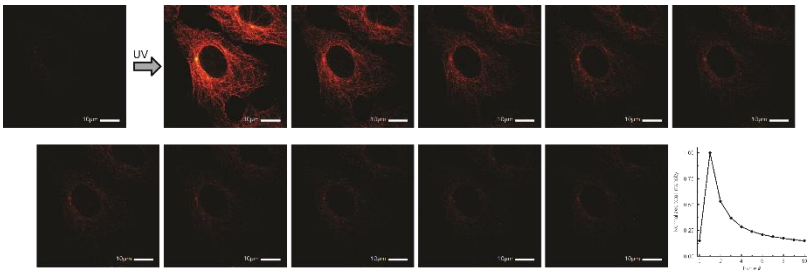

Figure S9. Confocal imaging of Vero cells immunostained with a secondary antibody labelled with compound **1**-CN,COMe (DOL 3.1) and a primary antibody against tubulin. The sample was first exposed to UV light with wide-field illumination, to switch-on the marker (OF→CF). Then, a series of then frames under identical conditions was recorded (top panel).

8. RESOLFT microscopy

RESOLFT images were recorded at a modified 1C RESOLFT QUAD Scanning microscope (Abberior Instruments, Göttingen) equipped with an 100x oil immersion objective (UPLSAPO XO, Olympus, 1.4 NA). The setup was originally built for dual color imaging in the red and green channel, which are separated by a dichroic mirror at a wavelength of 568 nm. Both channels were recorded in imaging and counts were added up. Laser powers used in imaging were measured in the back aperture of the objective. Power intensities were calculated with $I = P_{meas} / (\pi \cdot FWHM^2/4)$ for Gaussian shaped beams or with $I = P_{meas}/(2\pi R \cdot FWHM_{doughnut})$ with R as the radius of the doughnut peak around the PSF minimum in the center and $FWHM_{doughnut}$ as the FWHM of the doughnut PSF flanks. FWHM were either the calculated PSF FWHM (355 nm, $FWHM = 0.61 \cdot \lambda/NA$) or measured PSFs probed with reflective gold beads and FWHM obtained from Gaussian nonlinear curve fitting of 4 line profiles through the PSF center in the focal plane (488 nm Gaussian/doughnut-shaped). Intensities measured in the back aperture of the objective were reduced to 85 % for 488 nm or 50 % for 355 nm based on the transmission chart of the objective provided by the manufacturer.

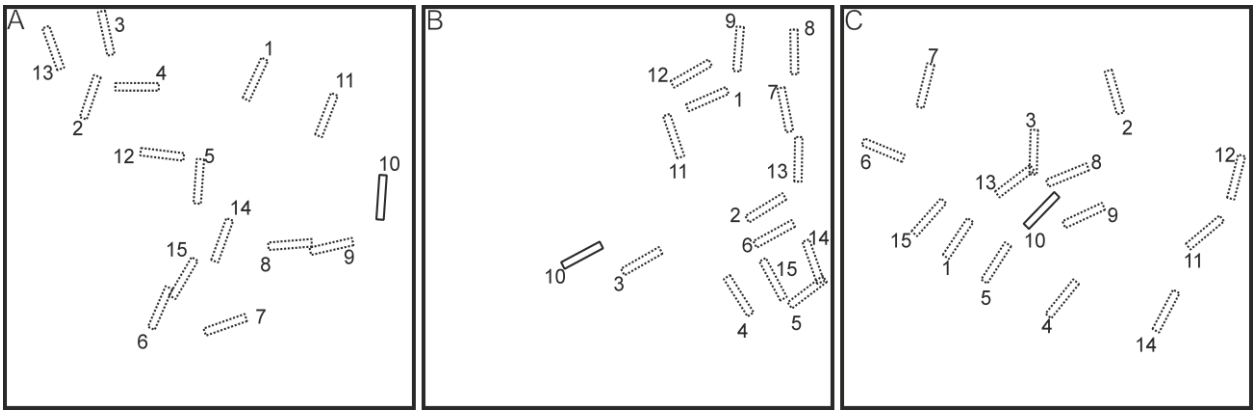

Figure S10. Line profile indices from Figure 4 (main text). The individual FWHM values from Lorentzian non-linear curve fitting are given in Table S2.

Table S2. Individual line profile FWHM from Figure 4 obtained from Lorentzian non linear curve fitting.

Line Profile	FWHM [nm]					
	1-MeO,COMe		**1**-CN,COMe		**1**-H,CH	
	Confocal	RESOLFT	Confocal	RESOLFT	Confocal	RESOLFT
1	174	77	174	103	156	92
2	188	61	212	97	184	100
3	188	73	211	128	185	62
4	175	81	166	128	157	88
5	166	64	141	117	232	135
6	186	59	180	80	219	116
7	183	98	178	77	187	102
8	200	70	217	82	193	105
9	159	71	129	97	152	101
10	198	75	189	97	196	96
11	204	109	218	94	171	95
12	181	91	218	105	156	85
13	198	63	190	92	208	91

14	194	86	173	89	162	104
15	164	64	204	76	192	125
Average	184	76	187	97	183	100
StDev	13	14	27	16	24	17

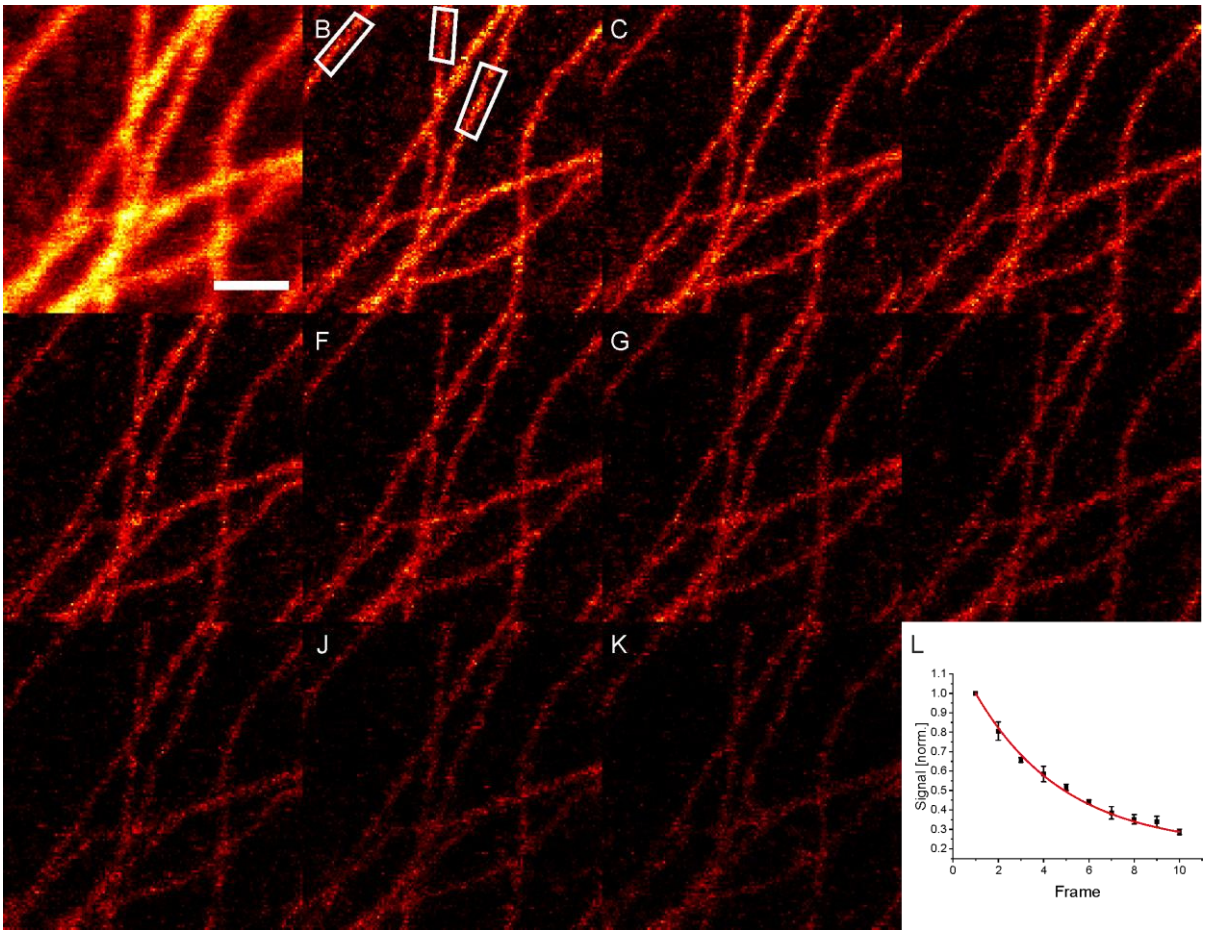

Figure S11. Confocal (A) and RESOLFT timelapse imaging over 10 frames (B-K) of fixed Vero cells immunostained with anti-tubulin primary antibodies and secondary antibodies labelled with **1**-MeO,COMe. Imaging parameters are stated in Table S3. Absolute counts in the boxed regions in B were calculated for all frames, normalized and fitted with an single exponential decay (L). 5 frames could be recorded before RESOLFT image brightness was reduced to 50 %. 30 nm pixel size, 1000 nm scale bar.

Table S3. Imaging parameters selected DAEs in RESOLFT timelapse imaging

Dye	355 nm	Pause	488 nm	Pause	488 nm

	activation [µs][a]	[µs]	Doughnut [µs][b]	[µs]	Readout [µs][d]
1-MeO,COMe			1500[b]		40
1-CN,COMe	175	200	1350[c]	100	120
1-H,CH			1350[c]		120

a) 361.9 W/cm²; b) 13.4 kW/cm²; c) 10.9 kW/cm²; d) 26.1 kW/cm². Confocal images were recorded only in the green channel without the breaks, 50 µs activation step and 40 µs readout prior to RESOLFT imaging.

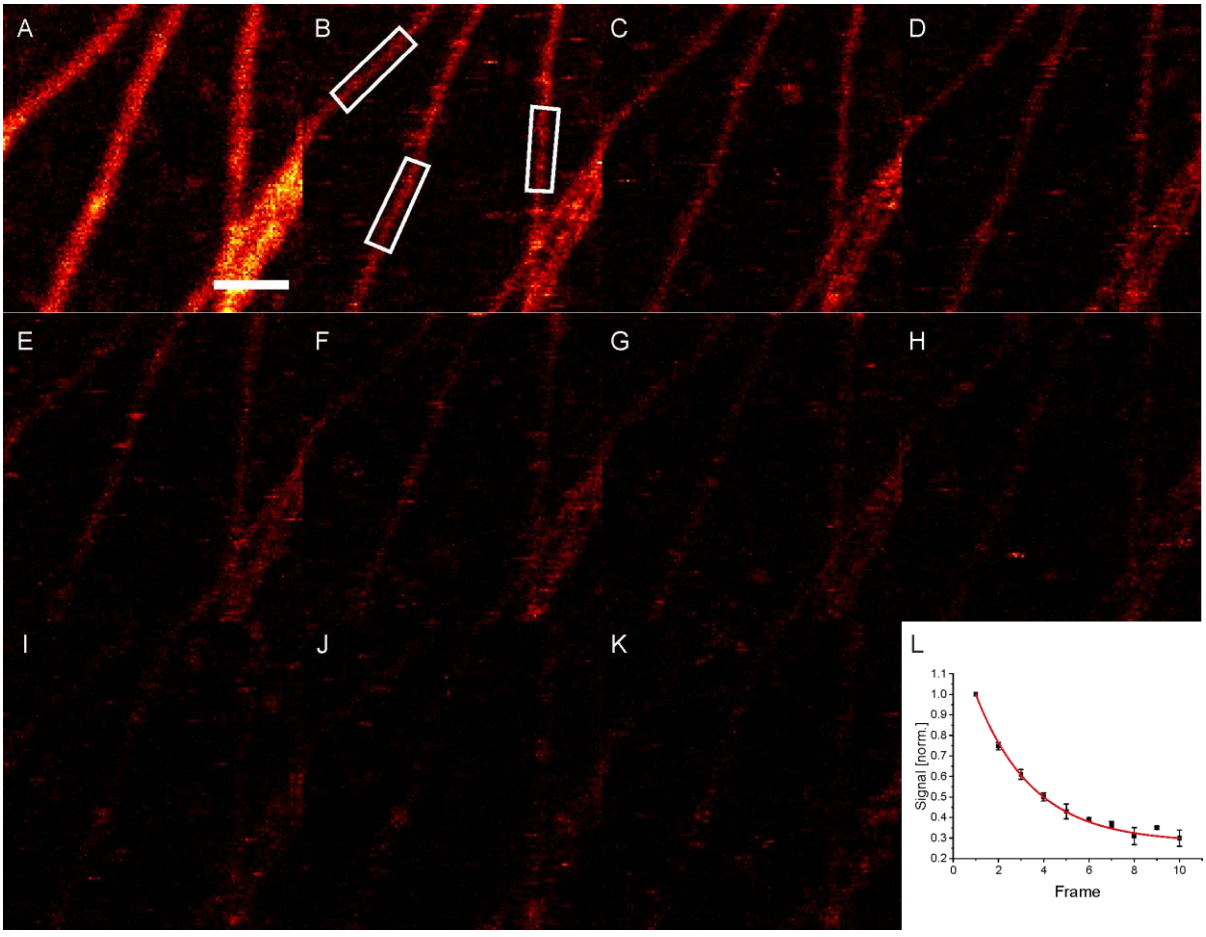

Figure S12. Confocal (A) and RESOLFT timelapse imaging over 10 frames (B-K) of fixed Vero cells immunostained with anti-tubulin primary antibodies and secondary antibodies labelled with **1**-CN,COMe. Imaging parameters are stated in Table S3. Absolute counts in the boxed regions in B were calculated for all frames, normalized and fitted with an single exponential decay (L). 4 frames could

be recorded before RESOLFT image brightness was reduced to 50 %. 30 nm pixel size, 1000 nm scale bar.

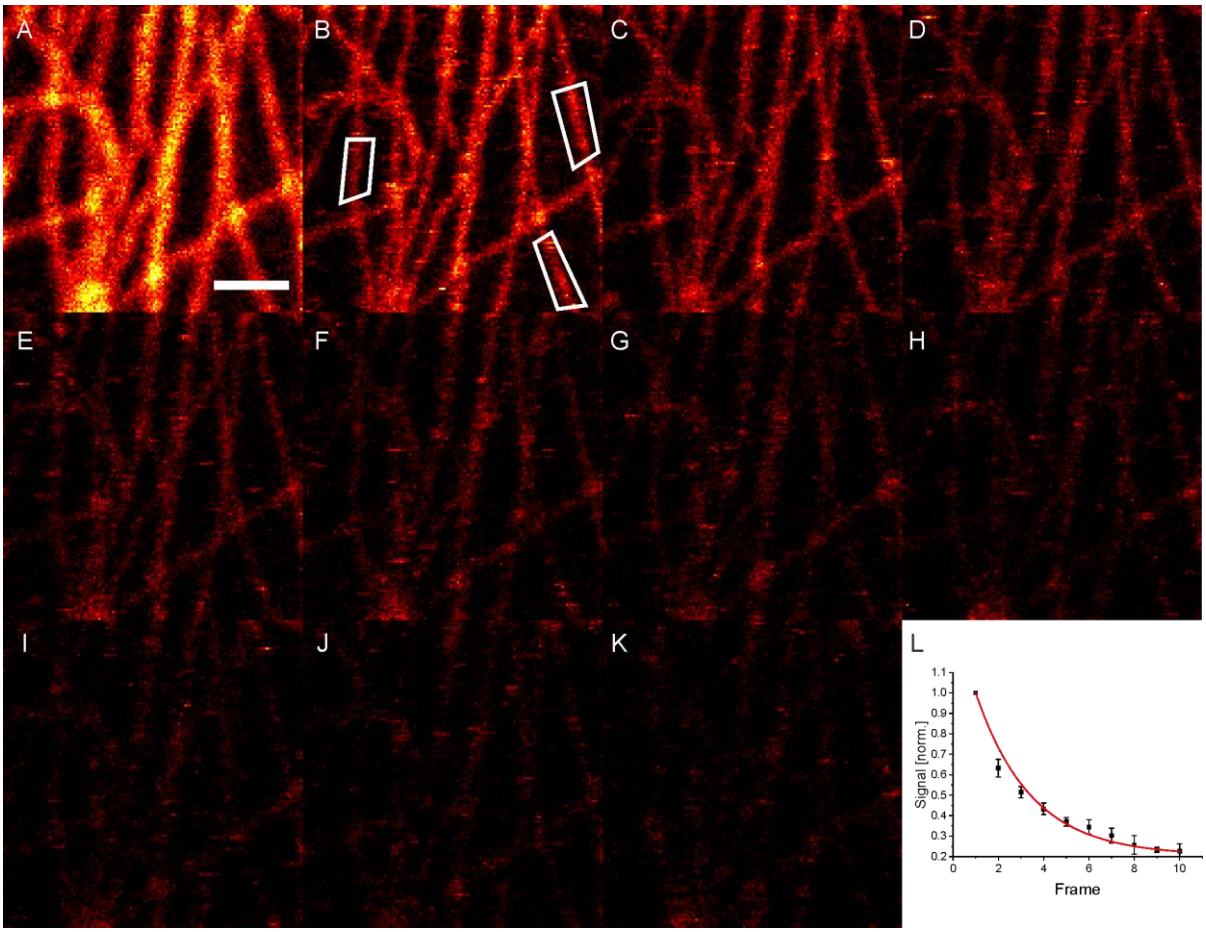

Figure S13. Confocal (A) and RESOLFT timelapse imaging over 10 frames (B-K) of fixed Vero cells immunostained with anti-tubulin primary antibodies and secondary antibodies labelled with **1**-H,CH. Imaging parameters are stated in Table S3. Absolute counts in the boxed regions in B were calculated for all frames, normalized and fitted with a single exponential decay (L). 3 frames could be recorded before RESOLFT image brightness was reduced to 50 %. 30 nm pixel size, 1000 nm scale bar.

Amino-modified polymer beads of 100 nm diameter (Micromer 01-01-102, Micromod Partikeltechnologie GmbH, Germany) were labelled with a similar protocol used to label proteins. Compound **1**-MeO,COMe (1.2 mg) in 120 µL of DMF was treated with under stirring with 1.1 equiv. of *N*-hydroxysuccinimide in DMF (2.5 µL) followed by slow addition of EDCI*HCl (7 equiv.) in DMF (70 µuL). After 15 min, the mixture was slowly added to 350 µL of the beads suspention (solid content 25 mg/mL), previously equilibrated with 40 µL of carbonate buffer (pH ≈ 8.1). The mixture was stirred in

the dark for one hour and then purified by centrifugation (3 times, 15000 g, 45 min each step), and finally re-suspended in water. The suspension was sonicated for about 10 minutes before sample mounting for imaging. Then, a dilution of 1/1000 was prepared in PVA 4% (in PBS), and spin coated onto cover slides for observation.

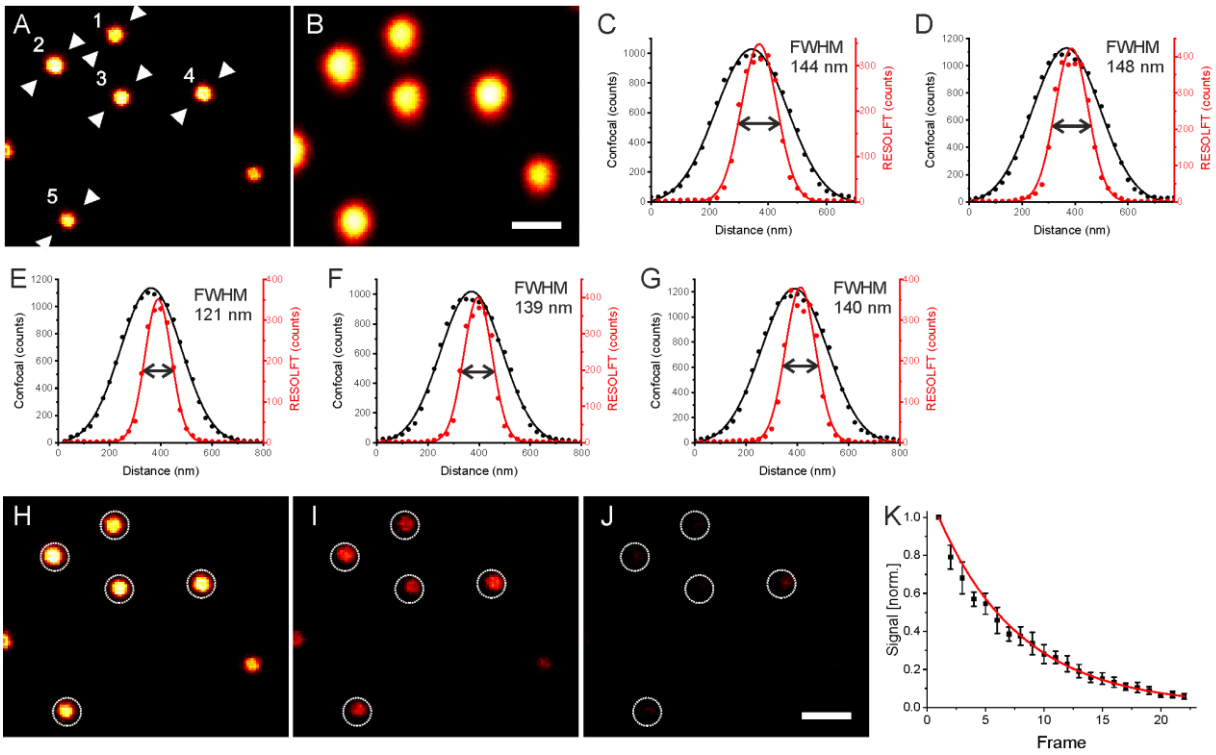

Figure S14. 100 nm polymer beads labelled with **1**-MeO,COMe were imaged in RESOLFT mode. Imaging parameters and powers are given in Table S4. Average optical resolution related to 5 beads in RESOLFT (A) and confocal (B) microscopy was analysed by Lorentzian non-linear curve fitting of line profiles measured over 2 adjacent lines (arrows) and resulted in an average FWHM of 137 and 292 nm, respectively. Individual line profiles with fits are shown in C-G for beads 1-5. The same region was imaged repeatedly in RESOLFT mode with the same imaging parameters, and frames 1 (H), 11 (I) and 22 (J) are shown. Absolute counts in the regions marked by circles in images H-J were measured, normalized and averaged. Data are shown in K with a single exponential decay non linear curve fit, showing that brightness of the beads was reduced to 50 % after about 7 frames. The confocal image was recorded only in the “green” channel. 25 nm pixel size, 500 nm scale bar.

Table S4. RESOLFT imaging parameters and observed FWHM for compound **1**-MeO,COMe attached to 100 nm beads in confocal and RESOLFT mode

Dye	355 nm activation [µs][a]	Pause [µs]	488 nm Doughnut [µs][b]	Pause [µs]	488 nm Readout [µs][c]	FWHM[d]	
						Confocal [nm]	RESOLFT [nm]
1-MeO,COMe	100	200	2000	40	20	292 ± 9	137 ± 10

a) 361.9 W/cm²; b) 12.8 kW/cm²; c) 30.7 kW/cm²; d) average FWHM of 5 line profiles measured over 2 adjacent lines and fitted by Gaussian non-linear curve fit. Confocal images were recorded without the breaks, 300 µs activation step and 40 µs readout prior to RESOLFT imaging.

Synthesis

Starting materials

All starting materials were purchased from TCI (Deutschland GmbH, Tokyo Chemical Industry Co.) and Sigma Aldrich and used without further purification. Tetra-*tert*-butyl 2, 2', 2'', 2'''-[(2-methoxy-5-(4, 4, 5, 5-tetramethyl-1, 3, 2-dioxaborolan-2-yl)isophthaloyl) bis (azanetriyl)] tetraacetate (B), tetra-*tert*-butyl 2, 2', 2'', 2'''-[[5-(4, 4, 5, 5-tetramethyl-1, 3, 2-dioxaborolan-2-yl) isophthaloyl] bis(azanetriyl)] tetraacetate (C), 3,3'-(perfluorocyclopent-1-ene-1, 2-diyl)bis(2-ethylbenzo[b]thiophene), and 3, 3'-(perfluorocyclopent-1-ene-1, 2-diyl)bis(2-ethylbenzo[b]thiophene 1, 1-dioxide) were prepared according to the published procedures (ref. 4 in the main text).

Electro spray ionization (ESI) mass-spectrometry (ESI-MS)

Low resolution ESI-MS were recorded on a *Varian 500-MS* spectrometer (Agilent). High resolution ESI-MS (HR ESI-MS) were recorded on a *MICROTOF* spectrometer (Bruker) equipped with an Apollo ion source and a direct injector with a LC-autosampler Agilent RR 1200.

Nuclear Magnetic Resonance (NMR)

NMR Spectra (^{1}H, ^{13}C and ^{19}F) were recorded on an *Agilent 400MR DD2* spectrometer. All ^{1}H- and ^{13}C-NMR spectra are referenced to the signals of the residual protons and ^{13}C in $CDCl_3$ (^{1}H: 7.26, ^{13}C: 77.00 ppm), CD_3CN (^{1}H: 1.94, ^{13}C: 1.32). Multiplicities of the signals are described as follows: s = singlet, br = broad, d = doublet, t = triplet, m = multiplet. Coupling constants *J* are given in Hz.

Preparation of boronic esters

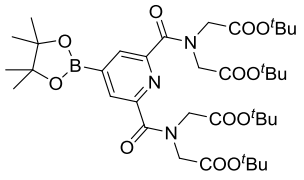

A

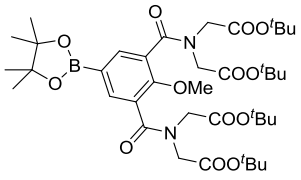

B

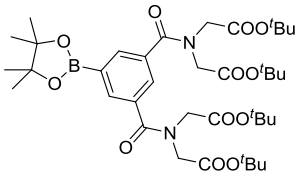

C

The synthesis of ester **A** is given in Scheme S1; esters B and C were prepared as described in ref. 4 (main text).

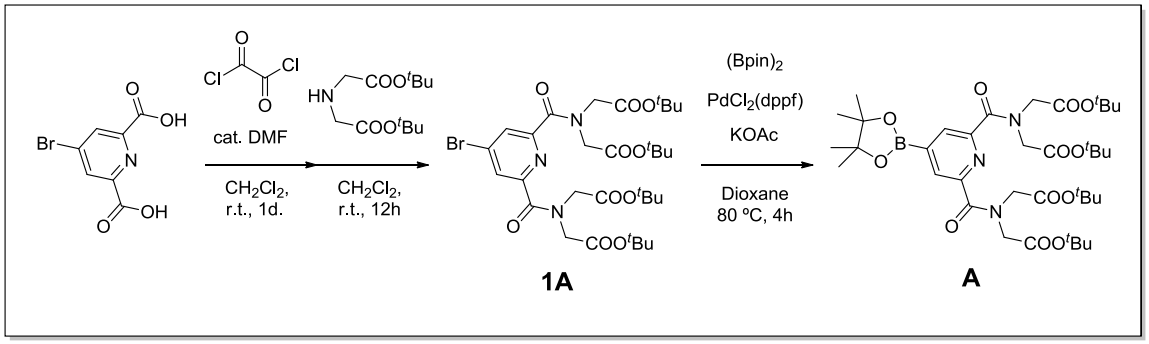

Scheme S1. Synthesis of tetra-*tert*-butyl-carboxylated pyridine boronic ester A

Tetra-*tert*-butyl 2,2',2'',2'''-((4-bromopyridine-2,6-dicarbonyl)bis(azanetriyl))-tetraacetate (1A)

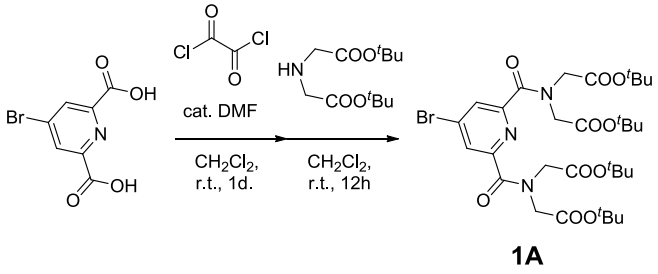

To a DCM (20 mL) containing suspension of 4-bromopyridine-2,6-dicarboxylic acid [4] (1.2 g, 4.9 mmol) was added DMF (5 drops, catalytic amount), and then oxalyl chroride (1.86 g, 1.46 mmol, 3.0 eq.) was slowly added at 0 ˚C. After stirring for one day at r.t., DCM and DMF was removed under vacuum to give a yellow powder. It was dissolved in DCM (20 mL) to which DCM (10 mL) containing TEA (0.50 mL, 3.6 mmol) and *di-tert*-butyl iminodiacetate (3.60 g, 14.7 mmol, 3.0 eq.) was added. The reaction solution was stirred overnight at r.t. under nitrogen atmosphere. Then the resulting mixture was washed with a saturated K_2CO_3 aq and brine, dried over $MgSO_4$ and concentrated under vacuum. The residue was purified by chromatography on a silica gel with a gradient eluent (*n*-hexane/EtOAc: 80/20 → 50/50). Recrystallization from a combined solution (*n*-hexane: DCM=10 : 1) afforded **1A** as white powder (2.4 g, 69% yield). R_f (*n*-hexane/EtOAc, 4/1, v/v) = 0.30. ^{1}H NMR (400 MHz, $CDCl_3$): δ (ppm) = 7.80 (s, 2 H), 4.20 (s, 4 H), 4.17 (s, 4 H), 1.48 (s, 18 H), 1.37 (s, 18 H). ^{13}C NMR (101 MHz, $CDCl_3$): δ (ppm) 167.7, 167.5, 167.1, 153.1, 146.4, 125.8, 82.4, 82.1, 77.3, 77.0, 76.7, 52.04, 49.7, 28.1, 27.9. ESI-MS, positive mode: m/z 722.2262 $[M+Na, ^{79}Br]^+$ (found), 724.2245 $[M+Na, ^{81}Br]^+$ (found), 722.2259 (calculated for $C_{31}H_{46}BrN_3NaO_{10}^+$, $[M+Na, ^{79}Br]^+$), 724.2248 (calculated for $C_{31}H_{46}BrN_3NaO_{10}$, $[M+Na, ^{81}Br]^+$).

tetra-*tert*-butyl 2,2',2'',2'''-((4-(4,4,5,5-tetramethyl-1,3,2-dioxaborolan-2-yl)pyridine-2,6-dicarbonyl)bis(azanetriyl))tetraacetate (A)

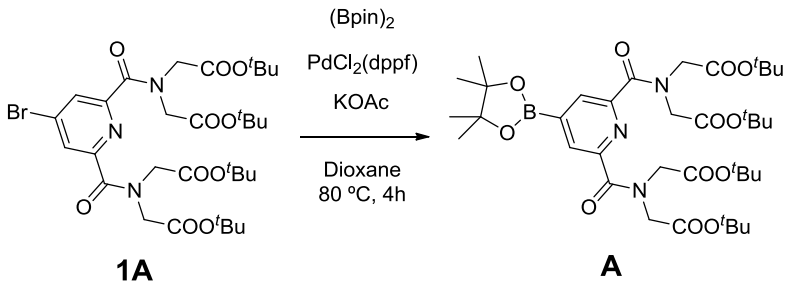

1A **A**

Into a flask flushed with N_2 was added compound **1A** (0.46 g, 0.66 mmol), bis-pinacolato diboron (0.20 g, 0.79 mmol, 1.2 eq.), KOAc (0.19 g, 1.97 mmol, 3.0 equiv.), and Pd(dppf)Cl_2 (30 mg, 0.041 mmol, 0.06 eq.). Dry 1,4-dioxan (7 mL) was added under N_2. The reaction mixture in a 50 mL flask was heated to 80˚C and stirred for 4 h. To the reaction mixture was added saturated brine (50 mL), it was extracted with DCM (2×50 mL), and the organic solution was then dried over $MgSO_4$. After concentrating under reduced pressure, the crude material was subjected to chromatography on silica gel with gradient elution with *n*-hexane/EtOAc (80/20 → 20/80) to afford the title compound **A** as a yellow solid (95 mg, 19%). R_f (*n*-hexane/EtOAc, 2/3,) = 0.0–0.3 (br). ^{1}H NMR (400 MHz, $CDCl_3$): δ (ppm) = 8.10 (s, 2 H), 4.23 (s, 4 H), 4.10 (s, 4 H), 1.48 (s, 18 H), 1.38 (s, 18 H), 1.30 (s, 12 H). ^{13}C NMR (101 MHz, $CDCl_3$): δ (ppm) = 168.6, 167.8, 167.8, 151.3, 130.2, 84.8, 82.2, 81.9, 51.9, 49.2, 28.1, 27.9, 24.8, 24.8. ESI-MS, positive mode: m/z = 770.4014 $[M+Na]^+$ (found), 770.4006 (calculated for $C_{37}H_{58}BN_3NaO_{12}^+$, $[M+Na]^+$).

Preparation of fluorescent diarylethenes 1-MeO,N, 1-MeO,COMe, 1-CN,N, 1-CN,COMe and 1-H,CH

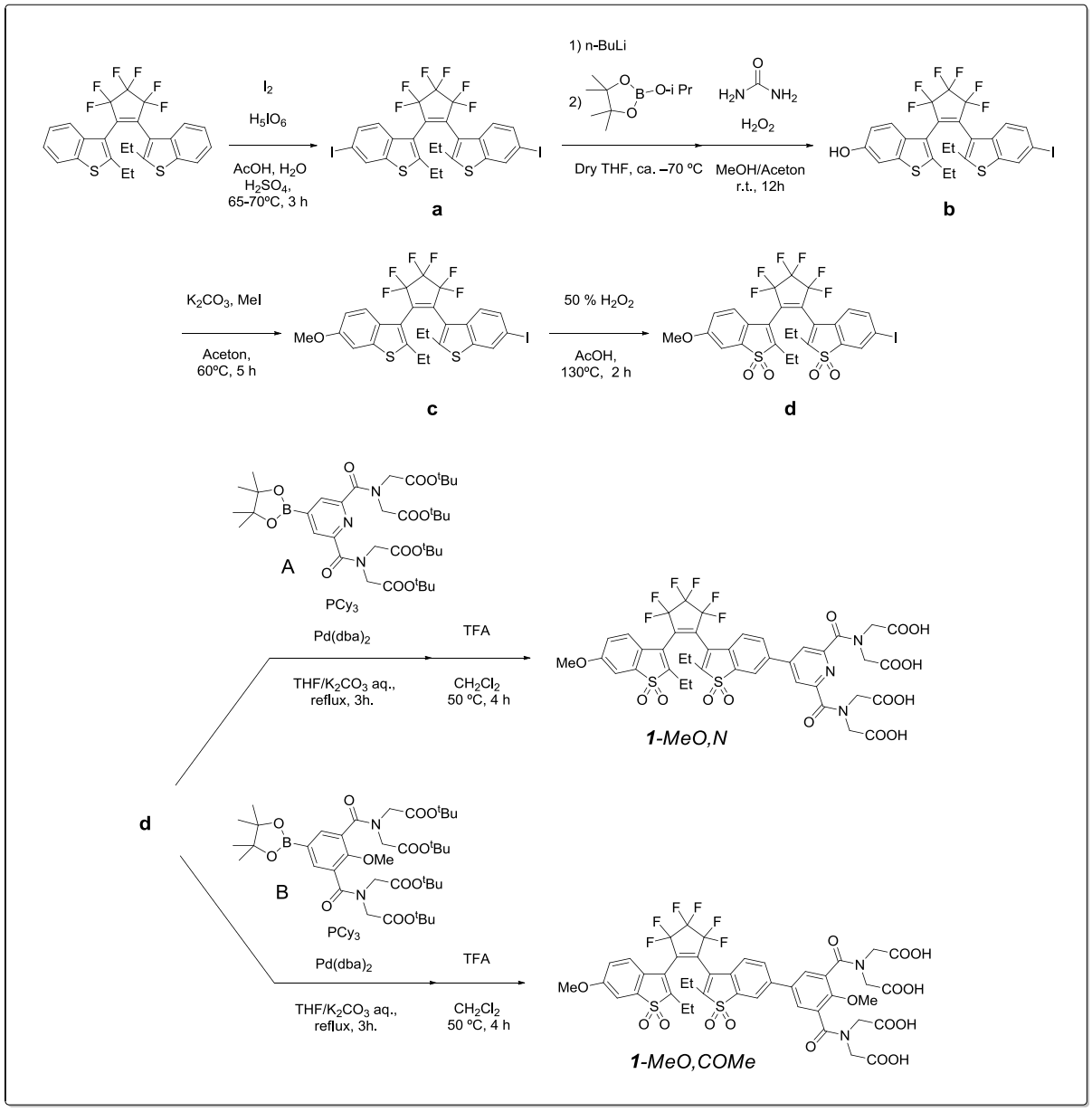

Scheme S2. Synthesis of **1**-MeO,N and **1**-MeO,COMe

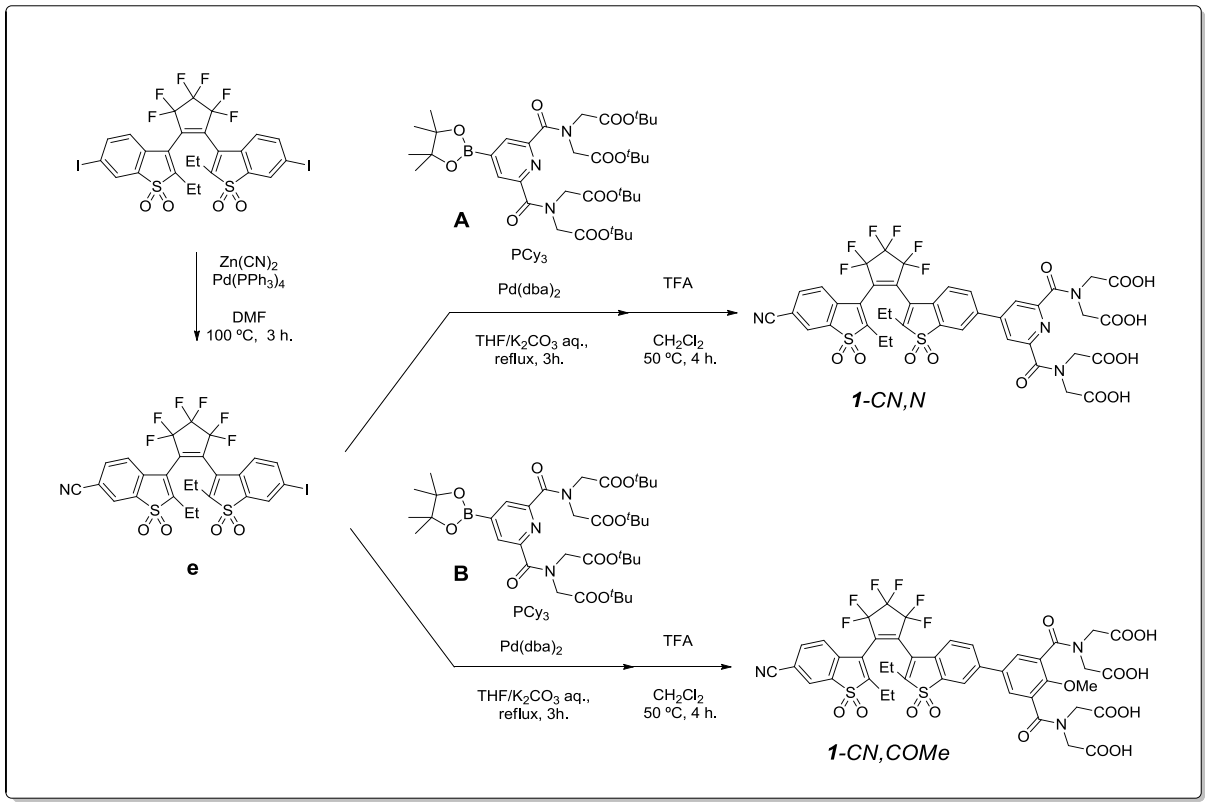

Scheme S3. Synthesis of **1**-CN,N and **1**-CN,COMe

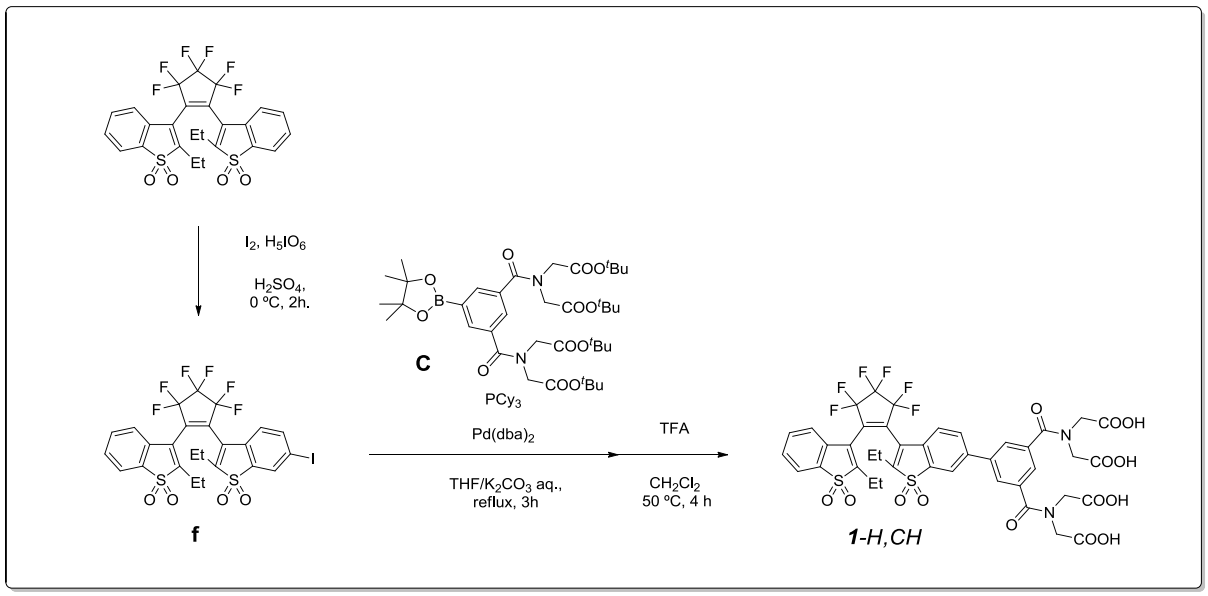

Scheme S4. Synthesis of **1**-H,CH

3,3'-(perfluorocyclopent-1-ene-1,2-diyl)bis(2-ethyl-6-iodobenzo[b]thiophene) (a)

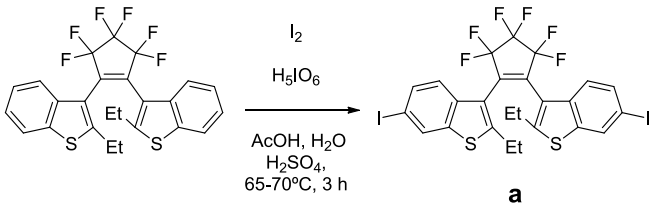

3,3'-(perfluorocyclopent-1-ene-1,2-diyl)bis(2-ethyl-6-iodobenzo[b]thiophene)[3] (4.5 g, 9.1 mmol) was suspended in a combined solution of AcOH (75 mL), H_2SO_4 (2.5 mL), and water (4 mL) and heated up to 65 ˚C in open air. A combined solid of iodine (2.53 g, 9.97 mmol, 1.1 equiv.) and H_5IO_6 (0.83 g, 3.6 mmol, 0.4 equiv.) was ground to fine powder and added to the reaction solution in 10 portions with 10 min intervals (total time 1 h 40 min). The reaction solution was further stirred for 80 min at 70 ˚C. After cooling down to r.t., the reaction mixture was added to water (300 mL). The formed solid was collected by filtration, and washed with water several times. The solid was dissolved in DCM (250 mL) which was then washed with conc. aq. NaOH (150 mL), conc. aq. $Na_2S_2O_3$ (150 mL), dried with $MgSO_4$ and concentrated. The obtained crude material was purified by column chromatography (*n*–hexane) and recrystallized twice from mixture of *n*-hexane/DCM (10/1) to yield compound **a** as a white solid (3.1 g, 46 %). R_f (*n*-hexane) = 0.33. *ap:p* = 2:1. ^{1}H NMR (400 MHz, $CDCl_3$): δ (ppm) = 8.06 (d, *J* = 1.2 Hz, 1.33 H, *ap*), 7.97 (d, *J* = 1.2 Hz, 0.66 H, *p*), 7.66 (dd, *J* = 8.4, 1.6 Hz, 1.33 H, *ap*), 7.48 (dd, *J* = 8.4, 1.6 Hz, 0.66 H, *p*), 7.37 (dd, *J* = 8.4, 2.0 Hz, 1.33 H, *ap*), 7.24 (dd, *J* = 8.4, 1.2 Hz, 0.66 H, *p*), 2.96–2.30 (m, 4 H), 1.28 (t, *J* = 7.6 Hz, 2 H, *p*), 0.84 (t, *J* = 7.6 Hz, 4 H, *ap*). ^{13}C NMR (101 MHz, $CDCl_3$): δ (ppm) = 151.2, 150.8, 140.0, 139.9, 137.5, 137.2, 133.6, 133.4, 130.8, 130.7, 123.4, 123.3, 123.2, 123.1, 117.7, 117.6, 115.9, 115.9, 110.0, 89.1, 88.9, 77.3, 77.0, 76.7, 23.2, 23.2, 22.9, 15.9, 15.4. ^{19}F NMR (367 MHz, $CDCl_3$): δ (ppm) = -110.3 (m, 4.0 F, *p/ap*), -132.7 (m, 2.0 F, *p/ap*). ESI-MS: ESI-MS, negative mode: m/z = 746.8592 $[M-H]^-$ (found), 746.8614 (calculated for $C_{25}H_{15}F_6I_2S_2^-$, $[M-H]^-$).

2-ethyl-3-(2-(2-ethyl-6-iodobenzo[b]thiophen-3-yl)-3,3,4,4,5,5-hexafluorocyclopent-1-en-1-yl)benzo[b]thiophen-6-ol (b)

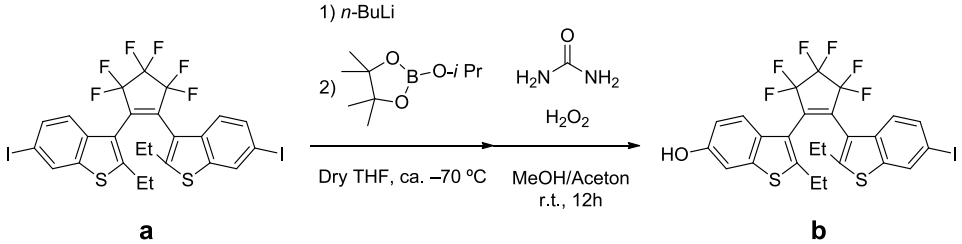

Compound a (4.0 g, 5.3 mmol) was dissolved in THF (20 ml) under N_2. *n*-BuLi (1.6 M in hexanes, 3.5 mL, 5.6 mmol, 1.0 eq.) was added at -70 ˚C with stirring, and the reaction solution was stirred for 30 min. 2-Isopropoxy-4,4,5,5-tetramethyl-1,3,2-dioxaborolane (1.4 g, 7.5mmol, 1.4 eq.) was added, and the reaction mixture was warmed to r.t. over 1 h. Water (50 mL) was added to the reaction solution, and it was extracted with DCM (50 mL, twice). The organic phase was separated, dried over $MgSO_4$, and concentrated under reduced pressure to give a crude boronic ester intermediate which was oxidized without further purification. The crude boronic ester was dissolved in the mixture of MeOH/Acetone (20 mL/5 mL) to which urea-hydrogen peroxide (0.75 g, 0.80 mmol, 1.5 eq.) was added in several portions at room temperature. After stirring for 12 h at r.t., sat. aq. NaCl was added. The reaction mixture was extracted with DCM (50 mL). The organic phase was separated, dried over $MgSO_4$, and concentrated under reduced pressure. Column chromatography with gradient elution (hexane/ethyl acetate = 85/15→ 60/40) afforded **compound b** as a white solid (1.6 g, 43 %). R_f (*n*-hexane/EtOAc, 3/2, v/v) = 0.6. *ap:p* = 2:1. ^{1}H NMR (400 MHz, $CDCl_3$): δ (ppm) = 8.05 (d, *J* = 1.6 Hz, 0.67 H, *ap*), 7.96 (d, *J* = 1.6 Hz, 0.33 H, *p*), 7.66 (dd, *J* = 8.8, 1.6 Hz, 0.67 H, *ap*), 7.50 (dd, *J* = 8.8, 2.0 Hz, 0.67 H, *ap*), 7.46 (dd, *J* = 8.4, 2.0 Hz, 0.33 H, *p*), 7.39 (dd, *J* = 8.8, 2.0 Hz, 0.67 H, a*p*), 7.35 (dd, *J* = 8.8, 1.6 Hz, 0.67 H, *p*), 7.26 (dd, *J* = 8.4, 1.6 Hz, 0.33 H, *p,* overlapped with $CHCl_3$ peak), 7.15 (d, *J* = 2.4 Hz, 0.67 H, a*p*), 7.06 (d, *J* = 2.4 Hz, 0.33 H, *p*), 6.92 (dd, *J* = 8.8, 2.4 Hz, 0.67 H, a*p*), 6.74 (dd, *J* = 8.8, 2.4 Hz, 0.33 H, *p*), 5.31–4.84 (br, 1 H), 2.97–2.27 (m, 4H), 1.32–1.22 (m, 2 H, *p*), 0.89–0.73 (m, 4 H, a*p*). ^{13}C NMR (101 MHz, $CDCl_3$): δ (ppm) = 153.1, 153.1, 151.1, 150.7, 147.8, 147.4, 140.90, 139.8, 139.6, 139.5, 137.6, 137.3, 133.6, 133.3, 132.4, 132.1, 130.7, 130.6, 124.7, 124.3, 123.5, 123.5, 123.4, 123.3, 123.0, 122.9, 122.7, 122.7, 122.2, 118.0, 117.8, 117.4, 117.2, 114.5, 114.4, 114.3, 110.0, 107.7, 107.6, 88.90, 88.8, 23.2, 23.2, 22.8, 15.9, 15.8, 15.4, 15.3. ^{19}F NMR (367 MHz, $CDCl_3$): δ (ppm) = -110.3 (m, 4.0 F, *p/ap*), -132.7 (m, 2.0 F, *p/ap*). ESI-MS: negative mode: m/z = 636.9582 $[M-H]^-$ (found), 636.9597 (calculated for $C_{25}H_{16}F_6IOS_2^-$, $[M-H]^-$).

2-ethyl-3-(2-(2-ethyl-6-iodobenzo[b]thiophen-3-yl)-3,3,4,4,5,5-hexafluorocyclopent-1-en-1-yl)-6-methoxybenzo[b]thiophene (c)

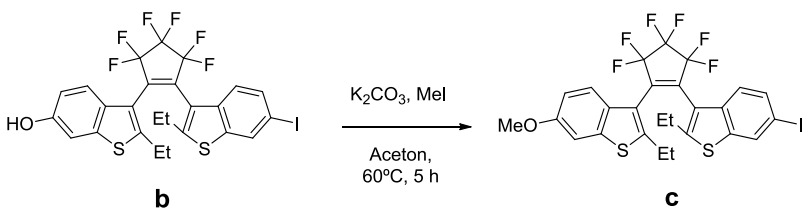

b **c**

Compound b (1.0 g, 1.6 mmol) was dissolved in dry acetone (20 mL) under N_2. Finely ground K_2CO_3 (2.0 g, 14 mmol, 9.0 eq.) and MeI (0.67 g, 4.7 mmol, 3.0 eq.) were added to the solution. The reaction solution was heated to 60 ˚C and stirred for 5h. After confirming the completing of the reaction by TLC, water (100 mL) was added, and the reaction mixture was extracted with DCM (50 mL, twice). The organic phase was collected, dried over $MgSO_4$, and concentrated under reduced pressure. The collected solid was washed with hexane to give compound **c** (0.92 g, 90 %) as a white solid. R_f (*n*-hexane/EtOAc, 4/1) = 0.53. *ap:p* = 2:1. ^{1}H NMR (400 MHz, $CDCl_3$): δ = 8.05 (d, *J* = 1.6 Hz, 0.67 H, *ap*), 7.96 (d, *J* = 1.6 Hz, 0.33 H, *p*), 7.76 (dd, *J* = 8.4, 1.6 Hz, 0.67 H, *ap*), 7.52 (dd, *J* = 8.8, 2.4 Hz, 0.67 H, *ap*), 7.45 (dd, *J* = 8.4, 2.4 Hz, 0.33 H, *p*), 7.43–7.35 (m, 1H), 7.26 (dd, *J* = 8.8, 1.6 Hz, 0.33 H, *p,* overlapped with CD_3Cl), 7.19 (d, *J* = 2.4 Hz, 0.67 H, a*p*), 7.11 (d, *J* = 2.4 Hz, 0.33 H, *p*), 7.00 (dd, *J* = 8.8, 2.4 Hz, 0.67 H, a*p*), 6.83 (dd, *J* = 8.8, 2.4 Hz, 0.33 H, *p*), 3.88 (s, 2 H, *ap*), 3.80 (s, 1 H, *p*), 1.35–1.21 (m, 2 H, *p*), 0.90–0.72 (m, 4 H, *ap*). ^{13}C NMR (101 MHz, $CDCl_3$): δ (ppm) = 157.3, 157.3, 151.2, 150.6, 147.6, 147.2, 140.0, 139.8, 139.6, 139.4, 137.6, 137.3, 137.3, 133.6, 133.3, 132.1, 131.8, 130.7, 130.6, 130.6, 123.5, 123.5, 123.4, 123.3, 122.8, 122.8, 122.72, 122.7, 122.6, 122.5, 117.9, 117.2, 114.6, 114.4, 110.0, 104.8, 104.8, 88.9, 88.8, 55.6, 55.5, 23.2, 23.2, 23.1, 23.1, 22.8, 16.0, 15.8, 15.5, 15.3. ^{19}F NMR (367 MHz, $CDCl_3$): ^{19}F NMR (367 MHz, $CDCl_3$): δ (ppm) = -110.3 (m, 4.0 F, *p/ap*), -132.7 (m, 2.0 F, *p/ap*). ESI-MS: negative mode: m/z = 650.9716 $[M-H]^-$ (found), 650.9753 (calculated for $C_{26}H_{18}F_6IOS_2^-$, $[M-H]^-$).

2-ethyl-3-(2-(2-ethyl-6-iodo-1,1-dioxidobenzo[b]thiophen-3-yl)-3,3,4,4,5,5-hexafluorocyclopent-1-en-1-yl)-6-methoxybenzo[b]thiophene 1,1-dioxide (d)

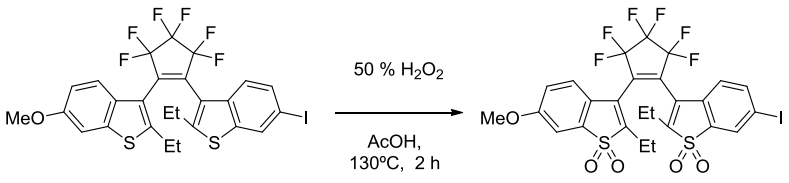

Compound c (0.12 g, 0.18 mmol) was dissolved in acetic acid (5 mL) and was heated to 130 ˚C. 50 % H_2O_2 (1 mL) was added, and the reaction mixture was further stirred with heating at 130 ˚C for 2 h. After cooling down to r.t., conc. aq. NaOH and aq. $Na_2S_2O_3$was. The mixture solution was then extracted by DCM (100 mL, three times). The organic phase was collected, dried over MgSO4, and concentrated under reduced pressure. The obtained crude material was purified by chromatography with DCM as eluent to give compound **d** as yellow solid (61 mg, 47 %). R_f (DCM) = 0.47. *ap:p* = 3:2. ^{1}H NMR (400 MHz, $CDCl_3$): δ = 8.05 (d, *J* = 1.6 Hz, 0.6 H, *ap*), δ (ppm) = 7.98 (d, *J* = 1.6 Hz, 0.4 H, *a*), 7.94

(dd, *J* = 8.0, 2.0 Hz, 0.6 H, *ap*), 7.76 (dd, *J* = 8.0, 2.0 Hz, 0.4 H, *p*), 7.28 (d, *J* = 1.6 Hz, 0.6 H, *ap*), 7.22 (d, *J* = 2.0 Hz, 0.4 H, *p*), 7.10–7.05 (m, 1 H), 7.00–6.80 (m, 2 H). ^{13}C NMR (101 MHz, $CDCl_3$): *δ* (ppm) = 162.0, 162.0, 148.2, 147.9, 146.6, 146.1, 142.7, 142.3, 137.4, 137.4, 136.9, 136.9, 133.8, 131.2, 131.1, 128.9, 128.8, 124.0, 124.0, 123.9, 123.8, 123.8, 123.7, 123.7, 123.4, 123.4, 123.4, 123.0, 122.9, 121.3, 121.3, 119.2, 110.0, 108.2, 108.1, 96.2, 96.2, 56.2, 56.1, 19.2, 19.1, 19.1, 19.0, 12.0, 11.8, 11.7, 11.4. ^{19}F NMR (367 MHz, $CDCl_3$): *δ* (ppm) = -110.0 (m, 4.0 F, *p/ap*), -132.2 (m, 2.0 F, *p/ap*). ESI-MS: negative mode: m/z = 714.9520 $[M-H]^-$ (found), 714.9550 (calculated for $C_{26}H_{18}F_6IO_5S_2^-$, $[M-H]^-$).

2-ethyl-3-(2-(2-ethyl-6-iodo-1,1-dioxidobenzo[*b*]thiophen-3-yl)-3,3,4,4,5,5-hexafluorocyclopent-1-en-1-yl)benzo[*b*]thiophene-6-carbonitrile 1,1-dioxide

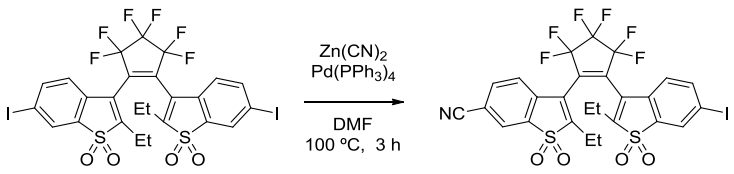

e

3,3'-(perfluorocyclopent-1-ene-1,2-diyl)bis(2-ethyl-6-iodobenzo[b]thiophene 1,1-dioxide)[4] (1.0 g, 1.2 mmol), $Pd(PPh_3)_4$ (0.25 g, 0.22 mmol, 0.18 eq.), and $Zn(CN)_2$ (0.25 g, 2.13 mmol, 1.8 eq.) were dissolved in dry DMF (7 mL) under N_2 atmosphere. The reaction mixture was heated to 100 ˚C for 3 h. DMF was removed under vacuum at 80 ˚C. After cooling to r.t., saturated aq. NaCl (100 mL) was added, and the reaction mixture was extracted with DCM (100 mL, twice).The organic phase was collected, dried over $MgSO_4$, and concentrated under reduced pressure. The resulting crude material was subjected to chromatography (DCM/Hexane, 8/2→10/0) to give **compound e** as pale yellow solid (0.31 g, 36 %). R_f (DCM, open-ring form) = 0.42. *ap:p* = 1:1. ^{1}H NMR (400 MHz, $CDCl_3$): *δ* (ppm) = 8.10–7.99 (m, 1. 4H), *δ* = 7.99–7.87 (m, 1.6 H), 7.79 (dd, *J* = 8.0, 1.6, 0.5 H, *ap*), 7.74 (dd, *J* = 8.0, 1.6 Hz, 0.5 H, *p*), 7.31 (d, *J* = 8.0 Hz, 0.5H, *ap*), 7.19 (d, *J* = 8.0 Hz, 0.5 H, *a*), 6.90 (d, *J* = 8.0 Hz, 0.5 H, *ap*), 6.80 (d, *J* = 8.0 Hz, 0.5 H, *p*), 2.74–2.23 (m, 4 H), 1.45–1.34 (m, 2.5 H), 1.13–1.01(m, 3.5 H). ^{13}C NMR (101 MHz, $CDCl_3$): *δ* (ppm) = 152.3, 151.9, 148.7, 148.0, 142.8, 142.4, 137.7, 137.4, 136.9, 136.8, 136.6, 136.6, 132.9, 132.8, 131.5, 131.4, 128.5, 128.5, 125.7, 123.8, 123.7, 123.7, 123.3, 123.2, 123.2, 122.8, 122.7, 122.4, 122.1, 122.0, 116.2, 115.0, 115.0, 96.6, 96.6, 53.4, 19.6, 19.5, 19.2, 19.1, 11.7, 11.7, 11.5, 11.4. ^{19}F NMR (367 MHz, $CDCl_3$): *δ* (ppm) = -109.9 (m, 4.0 F, *p/ap*), -132.0 (m, 2.0 F, *p/ap*). ESI-MS: negative mode: m/z = 709.9393 $[M-H]^-$ (found), 709.9397 (calculated for $C_{26}H_{15}F_6INO_4S_2^-$, $[M-H]^-$).

2-ethyl-3-(2-(2-ethyl-1,1-dioxidobenzo[*b*]thiophen-3-yl)-3,3,4,4,5,5-hexafluorocyclopent-1-en-1-yl)-6-iodobenzo[*b*]thiophene 1,1-dioxide

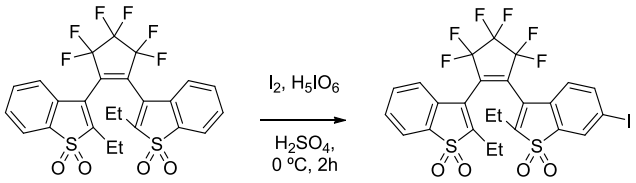

f

3,3'-(perfluorocyclopent-1-ene-1,2-diyl)bis(2-ethylbenzo[*b*]thiophene 1,1-dioxide)[4] (4.3 g, 7.7 mmol) was dissolved conc. H_2SO_4 (80 mL) and the solution was cooled to –0 ˚C in an ice bath. I_2 (1.9 g, 7.4 mmol, 0.97 eq.) and H_5IO_6 (0.90 g, 4.0 mmol, 0.52 eq.) were mixed together and ground to powder which was then added to the solution in several portions. After stirring for 2 h at 0 ˚C, the reaction solution was poured to crushed ice and stirred for another 2 h at r.t. The formed solid was filtered off, washed with hexane several times, and dried under high vacuum. The crude material was purified twice by column chromatography (n-hexane/EtOAc, 9/1→3/2) to give compound **f** as white powder (0.86 g, 16 %). R_f (DCM/Hexane = 9/1) = 0.30. ^{1}H NMR (400 MHz, $CDCl_3$): δ (ppm) = 8.10–7.85 (m, 1.6 H), 7.79–7.67 (m, 1.4 H), 7.65–7.53 (m, 1H), 7.53–7.40 (m, 1H), 7.19 (d, *J* = 6.8 Hz, 0.6H, *ap*), 7.08 (d, *J* = 7.6 Hz, 0.4 H, *p*), 2.73–2.25 (m, 4 H), 1.46–1.32 (m, 2.4 H), 1.16–0.95 (m, 3.6 H). ^{13}C NMR (101 MHz, $CDCl_3$): δ (ppm) = 148.7, 148.3, 148.2, 147.9, 142.7, 142.3, 136.9, 136.9, 135.6, 135.6, 133.9, 133.5, 131.2, 131.1, 130.9, 130.9, 129.4, 129.2, 128.9, 128.7, 123.9, 123.7, 123.2, 123.1, 122.9, 122.9, 122.7, 122.7, 122.5, 122.4, 122.4, 96.3, 96.2, 19.2, 19.1, 19.1, 11.9, 11.7, 11.6, 11.3. ^{19}F NMR (367 MHz, $CDCl_3$): δ (ppm) = -110.0 (m, 4.0 F, *p/ap*), -132.2 (m, 2.0 F, *p/ap*). ESI-MS: negative mode: m/z = 684.9422 $[M-H]^-$ (found), 684.9444 (calculated for $C_{25}H_{16}F_6IO_4S_2^-$, $[M-H]^-$).

Compound 1-MeO,N

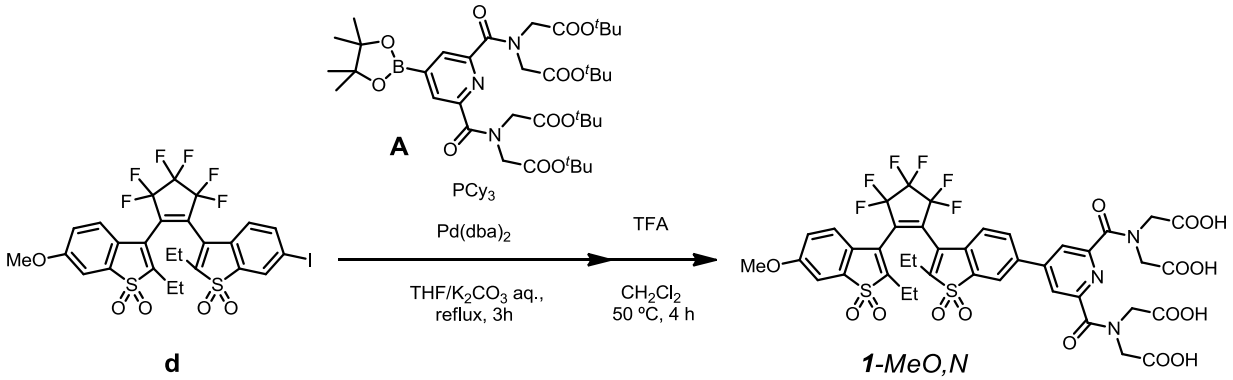

Anhydrous THF (10 ml) and sat. aq. K_2CO_3 (10 ml) were added to 25 mL flask flushed with N_2. To the vigorously stirring solution containing compound **d** (0.30 g, 0.42 mmol) and boronic ester **A** (0.36 g, 0.5 mmol, 1.2 eq.) was added PCy_3 20 wt. % in toluene (0.2 ml) and $Pd(dba)_2$ (60 mg, 0.10 mmol, 0.25 eq.). The reaction mixture was heated to reflux for 3 h. After cooling down to r.t., sat. aq. NaCl was added, and the reaction mixture was extracted with DCM (200 mL, twice). The organic solutions were collected, dried over $MgSO_4$, and concentrated under reduced pressure. The remaining dark solid was subjected to column chromatography (*n*-hexane/EtOAc, 9/1→7/3). The obtained crude material was added to a solution of DCM/TFA (5 mL/5 mL) and heated to 50 ˚C at 4 h. DCM and excess TFA were removed under vacuum to give yellow solid. Purification was carried out by reverse phase column chromatography (0.1% aq. TFA / CH_3CN, gradient from 7/3 to 3/7) followed by liophilization (deionized H_2O and 1,4-dioxane). **1**-MeO,N was obtained as white solid (0.13 g, 31%). ^{1}H NMR (400 MHz, CD_3CN): δ (ppm) = 8.24 (d, *J* = 1.6 Hz, 0.6 H, *ap*), 8.15 (m, 1.2 H, *p*), 8.14 (s, 1.2 H, *ap*), 8.09 (s, 0.8 H, *p*), 8.07 (dd, *J* = 12.0, 2.0 Hz ,0.6 H, *ap*), 7.92 (dd, *J* = 12.0, 2.0 Hz ,0.4 H, *p*), 7.56–7.49 (m, 1 H, *ap/p*), 7.42 (d, *J* = 2.4 Hz, 0.6 H, *ap*), 7.36–7.25 (m, 1.4 H, *ap/p*), 7.19 (dd, *J* = 8.4, 2.4 Hz ,0.6 H, *ap*), 7.03 (dd, *J* = 8.4, 2.4 Hz ,0.4 H, *p*), 4.45–4.25 (m, 8.0 H, *ap/a*), 3.89 (s, 1.8 H, *ap*), 3.79 (s, 1.2 H, *a*), 2.69–2.30 (m, 4.0 H, *ap/p*), 1.37–1.24 (m, 2.4 H), 1.03–0.88 (m, 3.6 H). ^{13}C NMR (101 MHz, CD_3CN): δ (ppm) = 172.3, 172.3, 171.9, 168.8, 168.8, 163.4, 163.2, 152.4, 152.4, 150.8, 150.6, 149.5, 149.5, 147.5, 147.3, 140.6, 140.4, 138.2, 137.9, 137.4, 137.3, 134.7, 134.3, 131.2, 131.0, 125.9, 125.9, 125.9, 125.9, 125.8, 125.8, 125.4, 125.4, 125.3, 125.3, 124.7, 124.7, 124.3, 123.9, 122.1, 122.0, 121.9, 121.6, 120.5, 120.3, 109.4, 109.2, 67.7, 57.2, 57.2, 52.7, 52.7, 50.7, 20.1, 20.0 (two peaks), 19.9, 19.9, 19.8, 12.5, 12.3, 12.2, 12.0. δ (ppm) = -110.5 (m, 4.0 F, *p/ap*), -131.9 (m, 2.0 F, *p/ap*). ESI-MS: positive mode: m/z = 986.1334 $[M+H]^+$ (found), 986.1330 (calculated for $C_{41}H_{34}F_6N_3O_{15}S_2^+$, $[M+H]^+$).

Compound 1-MeO,COMe

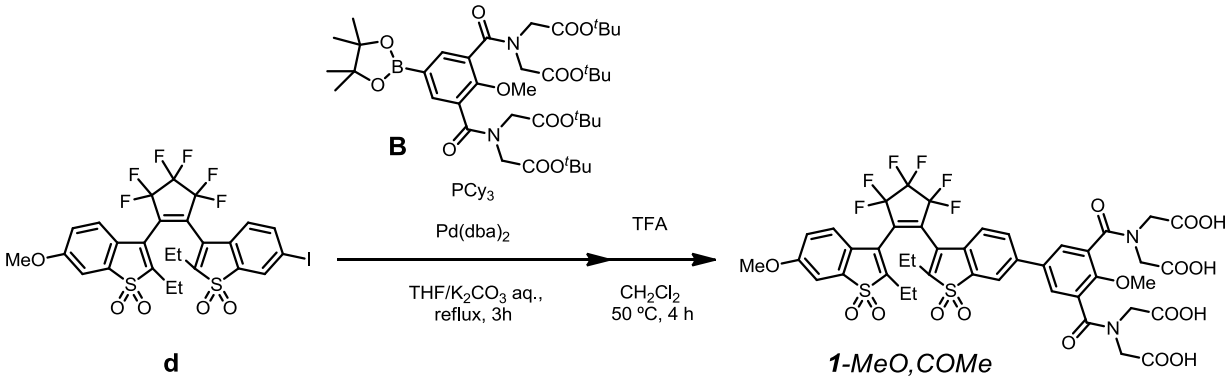

Anhydrous THF (5 ml) and sat. aq. K_2CO_3 (5 ml) were added to 25 mL flask flushed with N_2. To the vigorously stirring solution containing compound **d** (0.18 g, 0.25 mmol) and boronic ester **B** (0.30 g, 0.38 mmol, 1.5 eq.) was added added PCy_3 20 wt. % in toluene (0.1 ml) and $Pd(dba)_2$ (30 mg, 0.053 mmol, 0.21 eq.). The reaction mixture was heated to reflux for 3 h. After cooling down to r.t., sat. aq. NaCl was added and extracted by DCM (200 mL, twice). The organic solutions were collected, dried over $MgSO_4$, and concentrated under reduced pressure. The remaining dark solid was subjected to column chromatography (*n*-hexane/EtOAc, 9/1→7/3, v/v). The crude product was added to a solution of DCM/TFA (5 mL/5 mL) and heated to 50 ˚C for 4 h. DCM and excess of TFA were removed under vacuum to give yellow solid. Purification was carried out by reverse phase column chromatography (0.1% aq. TFA / CH_3CN, gradient from 7/3 to 3/7 followed by liophilization (deionized H_2O and 1,4-dioxane). **1**-MeO,COMe was obtained as white solid (93 mg, 37 %).^{1}H NMR (400 MHz, CD_3CN): δ (ppm) = 7.98 (d, *J* = 2.0 Hz, 0.6 H, *ap*), 7.89 (d, *J* = 2.4 Hz, 0.4 H, *p*), 7.86 (d, *J* = 8.0 Hz, 0.6H, *ap*), 7.72 (d, *J* = 8.4 Hz, 0.4 H, *p*), 7.59 (s, 1.2 H, *ap*), 7.54 (s, 0.8 H, *p*), 7.50–7.43 (m, 1.0 H, *ap/a*), 7.42 (d, *J* = 2.4 Hz, 0.6 H, *ap*), 7.36–7.26 (m, 1.4 H, *ap/a*), 7.19 (dd, *J* = 8.4, 2.4 Hz, 0.6 H, *ap*), 7.03 (dd, *J* = 8.4, 2.4 Hz, 0.4 H, *p*), 6.55–5.75 (br, 4 H, *ap/a*), 4.55–3.98 (m, 4 H, *ap/a*), 3.89 (s, 1.8 H, *ap*), 3.81 (s-br, 3.0 H, *ap/a*), 3.80 (s, 1.2 H, *a*), 2.67–2.30 (m, 4.0 H, *ap/a*), 1.38–1.25 (m, 2.4 H, *a*), 1.01–0.87 (m, 3.6 H, *ap*). ^{13}C NMR (101 MHz, CD_3CN): δ (ppm) = 170.3, 169.7, 168.8, 168.8, 162.3, 162.2, 148.8, 148.5, 146.5, 146.3, 141.8, 141.7, 137.2, 136.9, 136.3, 136.1, 132.8, 132.4, 128.5, 128.3, 128.0, 124.9, 124.8, 124.8, 124.3 (two peaks), 124.2 (two peaks), 124.2, 123.3 (two peaks), 123.1, 120.9, 120.6, 120.3, 120.1, 119.5, 119.1, 108.3, 108.3, 56.2, 56.17, 51.0 (two peaks), 48.0, 19.0, 18.9, 18.8, 18.7, 11.5, 11.4, 11.2, 11.0. ^{19}F NMR (101 MHz, CD_3CN) δ (ppm) = -110.5 (m, 4.0 F, *p/ap*), -131.9 (m, 2.0 F, *p/ap*). ESI-MS: negative mode: m/z = 1013.1315 $[M-H]^-$ (found), 1013.1338 (calculated for $C_{43}H_{35}F_6N_2O_{16}S_2$, $[M-H]^-$).

Compound 1-CN,N

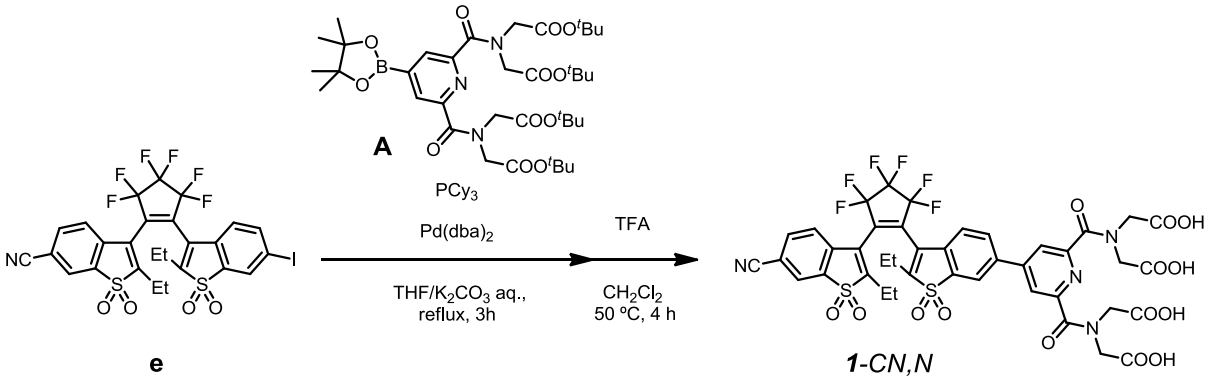

Anhydrous THF (10 mL) and sat. aq. K_2CO_3 (10 mL) were added to 25 ml flask and flushed with N_2. To the vigorously stirring solution containing compound **e** (0.24 mg, 0.34 mmol) and boronic ester **A** (0.40 g, 0.54 mmol, 1.6 eq.) was added PCy_3 20 wt. % in toluene (0.2 mL) and $Pd(dba)_2$ (60 mg, 0.10 mmol, 0.25 eq.). The reaction mixture was heated to reflux for 3 h. After cooling back to r.t., sat. aq. NaCl was added and extracted by DCM (200 mL, twice). The organic solutions were collected, dried over $MgSO_4$, and concentrated under reduced pressure. The remaining dark solid was subjected to column chromatography (*n*-hexane/EtOAc, 9/1→7/3). The crude product was added to a solution of DCM/TFA (5 mL/5 mL) and heated to 50 ˚C for 4 h. DCM and excess of TFA were removed under high vacuum to give yellow solid. Purification was carried out by reverse phase column chromatography (0.1% aq. TFA / CH_3CN, gradient from 7/3 to 3/7) followed by liophilization (deionized H_2O and 1,4-dioxane). **1**-CN,N was obtained as white solid (77 mg, 23%). ESI-MS: negative mode: *m/z* = 979.1006 $[M-H]^-$ (found), 979.1031 (calculated for $C_{41}H_{29}F6N_4O_{14}S_2$, $[M-H]^-$). ^{1}H NMR (400 MHz, CD_3CN): δ (ppm) = 8.23 (d, *J* = 2.0 Hz, 0.6H, *ap*), 8.20 (d, *J* = 0.4 Hz, 0.4 H, *p*), 8.18–8.12 (m, 1.8 H, *ap/p*), 8.10 (m, 1.2 H, *ap*), 8.09–8.04 (m, 1.0 H, *ap/p*), 7.95–7.88 (m, 1.0 H, *ap/p*), 7.61–7.52 (m, 1.6 H, *ap/p*), 7.47 (d, 8.0 H, *p*), 6.65–5.45 (s-br, 8.0 H, *p*), 4.40–4.27 (m, 8.0 H, *ap/p*), 2.73–2.32 (m, 4.0 H, *ap/p*), 1.38–1.30 (m, 2.4 H, *ap/p*), 1.03–0.94 (m, 3.6 H, *ap/p*). ^{13}C NMR (101 MHz, CD_3CN): δ (ppm) = 172.3, 171.9, 171.9, 168.8, 168.8, 152.8, 152.6, 152.4, 152.4, 151.1, 151.0, 150.7, 149.5, 149.4, 140.7, 140.5, 140.0, 139.9, 137.4, 137.2, 136.9, 136.7, 134.7, 134.4, 133.7, 133.7, 133.5, 133.5, 131.0, 130.8, 126.8, 126.6, 125.4, 125.4, 125.4, 125.3, 125.3, 125.1 (two peaks), 124.8, 124.7, 123.6 (two peak), 123.5, 122.2, 122.1, 117.7, 115.8, 115.6, 52.7, 52.7, 50.7, 20.2, 20.1, 20.0, 12.3, 12.2, 12.0, 11.9. ^{19}F NMR (101 MHz, CD_3CN) δ (ppm) = -110.3 (m, 4.0 F, *p/ap*), -131.6 (m, 2.0 F, *p/ap*). ESI-MS: negative mode: m/z = 979.1006 $[M-H]^-$ (found), 979.1031 (calculated for $C_{41}H_{29}F_6N_4O_{14}S_2$, $[M-H]^-$).

Compound 1-CN,COMe

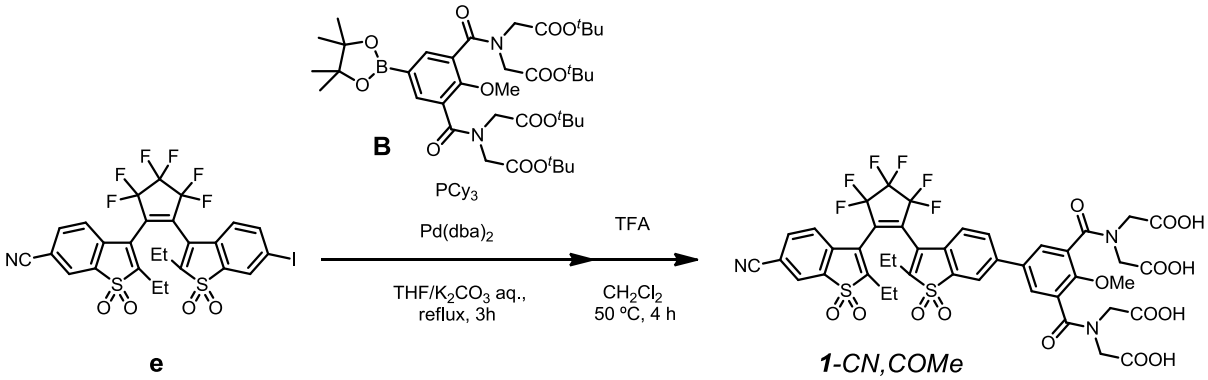

Anhydrous THF (7 mL) and sat. aq. K_2CO_3 (7 mL) were added to 25 mL flask flushed with N_2. To the vigorously stirring solution containing compound **e** (0.12 g, 0.17 mmol) and boronic ester ester **B** (0.20 g, 0.25 mmol, 1.5 eq.) was added added PCy_3 20 wt. % in toluene (0.2 mL) and $Pd(dba)_2$ (30 mg, 0.05 mmol, 0.30 eq.). The reaction mixture was heated to reflux for 3 h. After cooling down to r.t., sat. aq. NaCl was added, and the reaction mixture was extracted with DCM (200 mL, twice). The organic solutions were collected, dried over $MgSO_4$, and concentrated under reduced pressure. The remaining dark solid was subjected to column chromatography (*n*-hexane/EtOAc, 9/1→7/3). The crude product was added to a solution of DCM/TFA (5 mL/5 mL) and heated at 50 ˚C for 4 h. DCM and excess of TFA were removed under high vacuum to give yellow solid. Purification was carried out by reverse phase column chromatography (0.1% aq. TFA / CH_3CN, gradient from 7/3 to 3/7) followed by liophilization (deionized H_2O and 1,4-dioxane). **1**-CN,COMe was obtained as a white solid (46 mg, 27 %).^{1}H NMR (400 MHz, CD_3CN): δ (ppm) = 8.20 (d, *J* = 1.6 Hz, 0.6H, *ap*), 8.11 (d, *J* = 1.6 Hz, 0.4H, *p*), 8.07 (dd, *J* = 1.6, 8.0 Hz, 0.6H, *ap*), 7.98 (s, 0.6H, *ap*), 7.92 (d, *J* = 8.0 Hz, 0.4H, *p*), 7.89 (s, 0.4H, *p*), 7.86 (d, *J* = 8.0 Hz, 1.2H, *ap*), 7.70 (d, *J* = 8.0 Hz, 0.8H, *p*), 7.64–7.35 (m, 5.0H, *ap/p*), 6.08–5.59 (br, 4.0H, *ap/p*), 4.47–4.03 (m, 8.0H, *ap/p*), 3.85–3.75 (ss, 3.0H, *ap/p*), 2.74–2.31 (m, 4.0H, *ap/p*), 1.37–1.30 (m, 2.4H, *p*), 1.00–0.92 (m, 3.6H, *ap*). ^{13}C NMR (101 MHz, CD_3CN): δ (ppm) = 171.5, 171.4, 170.8, 169.8, 169.8, 152.7 (two peaks), 152.6, 150.0, 150.0, 149.7, 149.7, 143.0 (three peaks), 139.8, 137.2, 137.0, 136.9, 136.7, 133.9, 133.8, 133.7, 133.5 (two peaks), 131.0, 130.7, 129.6, 129.6, 129.1, 128.9, 126.8, 126.6, 125.4, 125.4, 125.3 (two peaks), 125.2, 125.1, 123.9, 123.8, 123.6, 123.5, 122.5, 122.1, 121.4, 121.3, 119.7, 117.7 (two peaks), 115.7, 115.6, 52.0, 49.2, 49.1, 49.1, 49.1, 49.0, 20.2, 20.2, 20.0, 19.9, 12.4, 12.2, 12.1, 11.9. ^{19}F NMR (367 MHz, CD_3CN) δ (ppm) = -110.3 (m, 4.0 F, *p/ap*), -131.7 (m, 2.0 F, *p/ap*). ESI-MS: negative mode: m/z = 1008.1148 $[M-H]^-$ (found), 1008.1185 (calculated for $C_{43}H_{32}F_6N_3O_{15}S_2$, [M-H]).

Compound *1*-*H,CH*

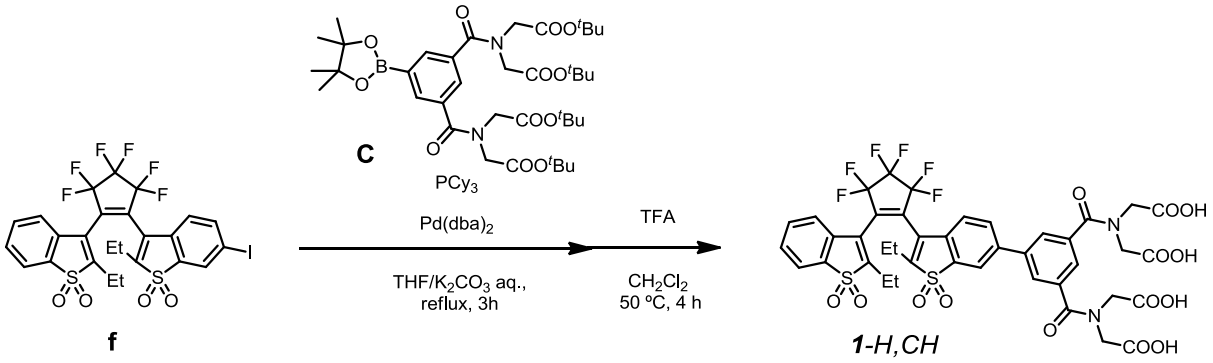

Anhydrous THF (10 mL) and sat. aq. K_2CO_3 (10 mL) were added to 25 mL flask and flushed with N_2. To the vigorously stirring solution containing **f** (0.50 g, 0.73 mmol) and boronic ester **C** (0.70 g, 0.95 mmol, 1.3 eq.) was added PCy_3 20 wt. % in toluene (0.2 ml) and Pd(dba)2 (60 mg, 0.10 mmol, 0.25 eq.). The reaction mixture was heated to reflux for 3 h. After cooling back to r.t., sat. aq. NaCl was added, and the reaction mixture extracted with DCM (200 mL, twice). The organic solutions were collected, dried over $MgSO_4$, and concentrated under reduced pressure. The remaining dark solid was subjected to column chromatography (*n*-hexane/EtOAc, 2/8→7/3, v/v). The crude product was added to a solution of DCM/TFA (20 mL/20 mL) and heated to 50 ˚C for 4 h. DCM and excess of TFA were removed under vacuum to give yellow solid. Purification was carried out by reverse phase column chromatography (0.1% aq. TFA / CH_3CN, gradient from 2/8 to 3/7) followed by liophilization. **1**-H,CH was obtained as white solid (0.28 g, 40 %). ^{1}H NMR (400 MHz, CD_3CN): δ (ppm) = 8.06 (d, *J* = 1.5 Hz, 0.6H, *ap*), 7.97 (d, *J* = 1.5 Hz, 0.4H, *p*), 7.93 (dd, *J* = 1.5, 8.0 Hz, 0.6H, *ap*), 7.82 (dd, *J* = 1.0, 7.5 Hz, 0.6H, *ap*), 7.78 (dd, *J* = 1.5, 8.0 Hz, 0.4H, *a*), 7.76 (d, *J* = 1.5 Hz, 1.2 H, *ap*), 7.75–7.70 (m, 1.2 H, *p*),7.69 (d, *J* = 1.5 Hz, 0.8 H, *p*), 7.66 (dt, *J* = 0.5, 7.5 Hz, 0.6 H, *ap*), 7.56–7.48 (m, 2.4 H, *ap/p*), 7.45 (s, 0.6 H, *ap*), 7.43 (s, 0.4 H, *a*), 7.42–7.35 (m, 1.6H, *ap/p*), 4.23 (s, 2.4 H, *ap*), 4.22 (s, 1.6 H, *a*), 4.13 (s, 2.4 H, *ap*), 4.10 (s, 1.6 H, *a*), 2.72–2.32 (m, 4.0 H, *ap/p*), 1.33 (m, 2.4 H, *p*), 0.94 (m, 3.6 H, *ap*), 8.10–6.90 (br, 4.0 H, *ap/p*). ^{13}C NMR (126 MHz, CD_3CN) δ (ppm) = 171.9 (two peaks), 171.6, 170.8, 150.1, 149.8, 149.5, 149.4, 143.2, 143.0, 141.4, 141.2 (two peaks), 141.1, 141.0, 140.9 (two peaks), 140.8, 140.3, 140.1, 137.5, 137.5, 137.2, 137.1, 136.2, 136.0, 135.7, 135.4, 134.3, 133.8, 132.4, 132.3, 130.1, 129.7, 129.7, 129.5, 127.9, 127.8, 125.9, 125.4 (two peaks), 125.2, 124.8, 124.7, 124.6, 124.6, 124.3, 124.1, 124.0, 123.0, 122.8, 121.8, 121.6, 52.7, 49.2, 19.9 (two peaks), 19.9, 19.8, 12.4, 12.3, 12.1, 12.0. ^{19}F NMR (367 MHz, CD_3CN) δ (ppm) = -110.3 (m, 4.0 F, *p/ap*), -131.8 (m, 2.0 F, *p/ap*) ESI-MS: negative mode: m/z = 953.1114 $[M-H]^-$ (found), 953.1126 (calculated for $C_{41}H_{31}F_6N_2O_{14}S_2^-$, $[M-H]^-$).

NMR spectra of compound 1A

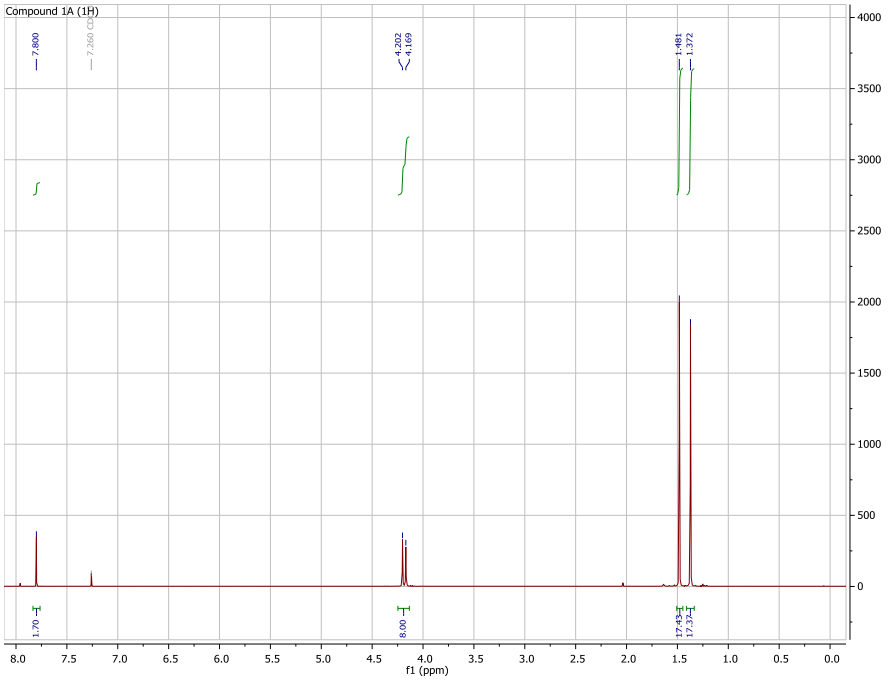

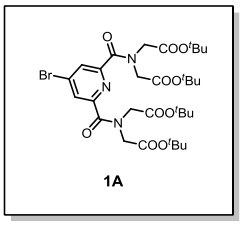

S

Figure S15-a. ^{1}H-NMR (400 MHz) chart of **1A** in $CDCl_3$

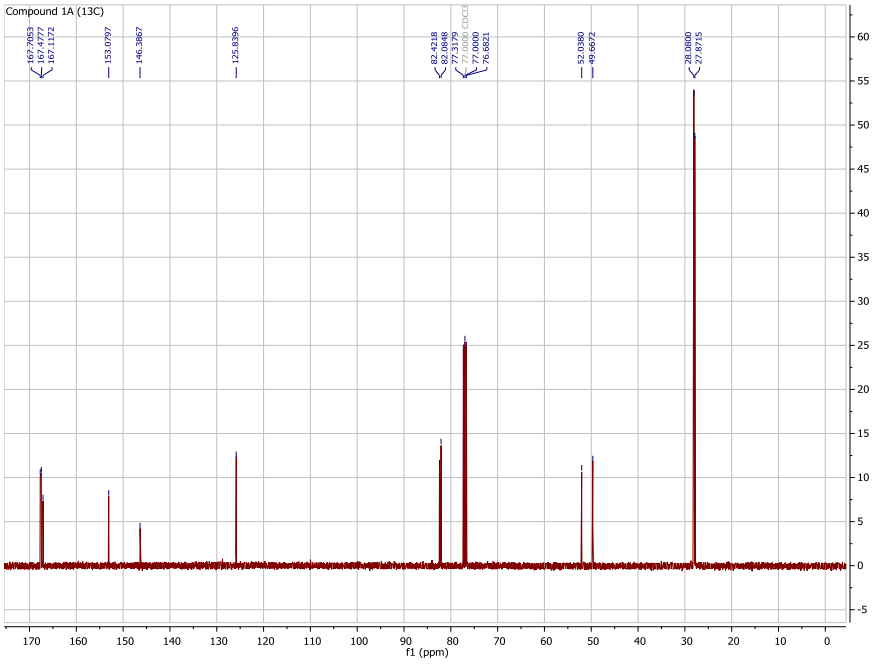

Figure S15-b. ^{13}C-NMR (101 MHz) chart of **1A** in $CDCl_3$

NMR spectra of compound A

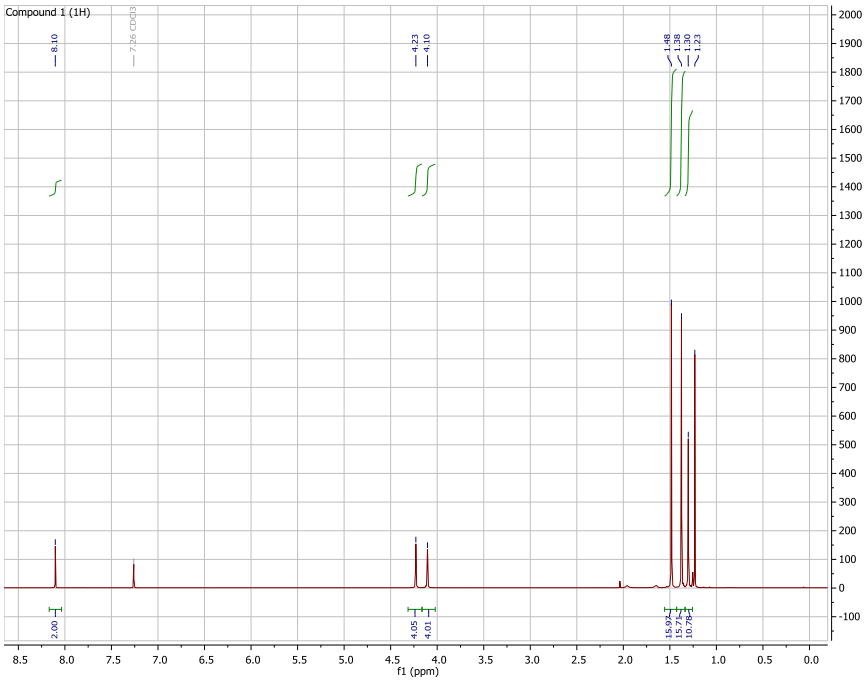

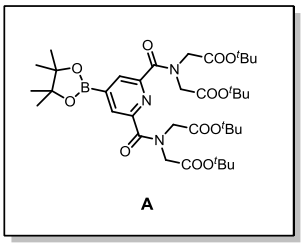

Figure S16-a. ^{1}H-NMR (400 MHz) chart of **A** in $CDCl_3$

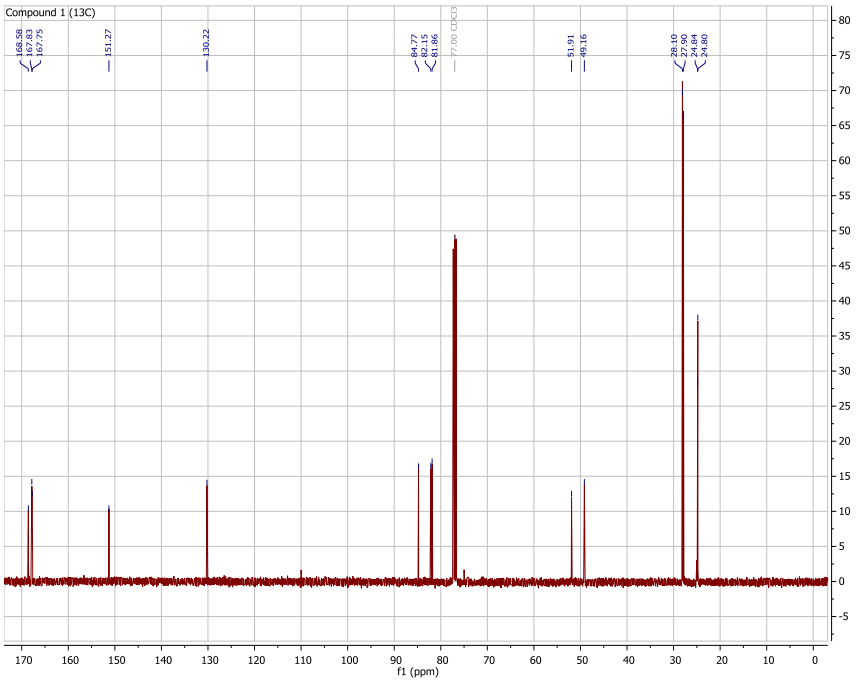

Figure S16-b. ^{13}C-NMR (101 MHz) chart of **A** in $CDCl_3$

NMR spectra of compound a

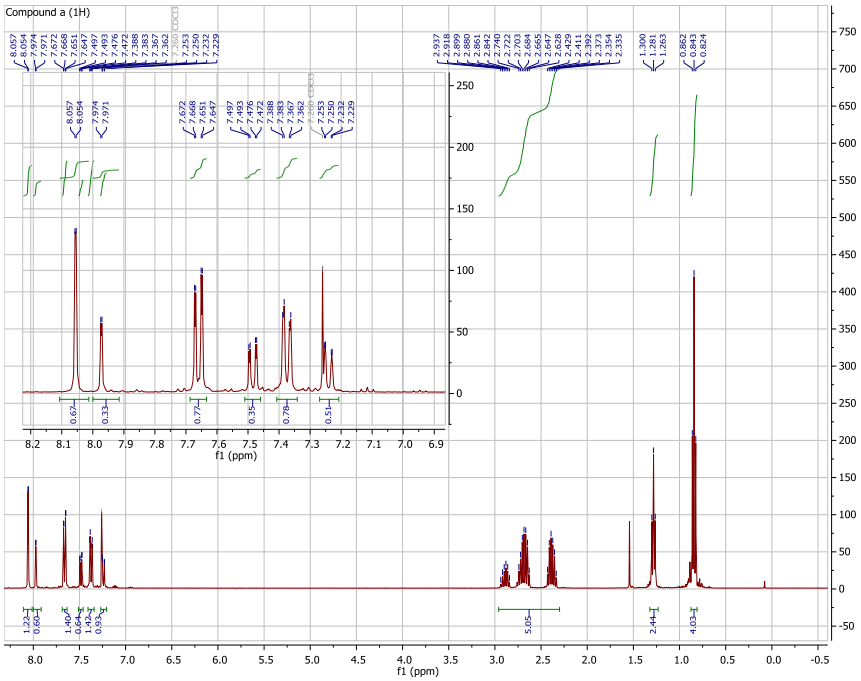

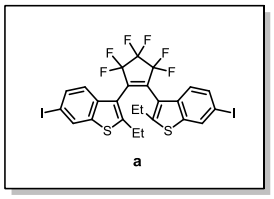

Figure S17-a. ^{1}H-NMR (400 MHz) chart of **a** in $CDCl_3$

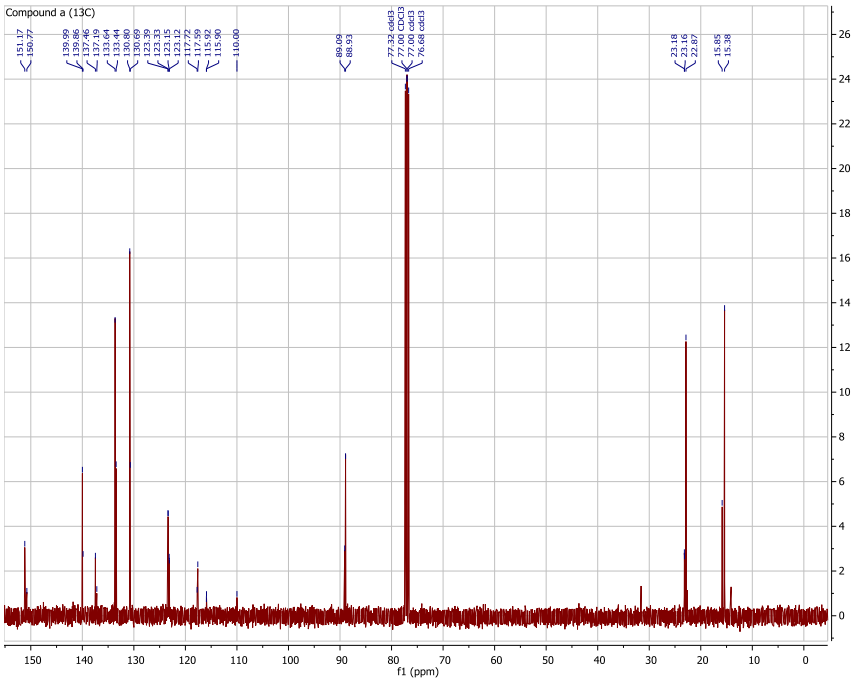

Figure S17-b. ^{13}C-NMR (101 MHz) chart of **a** in $CDCl_3$

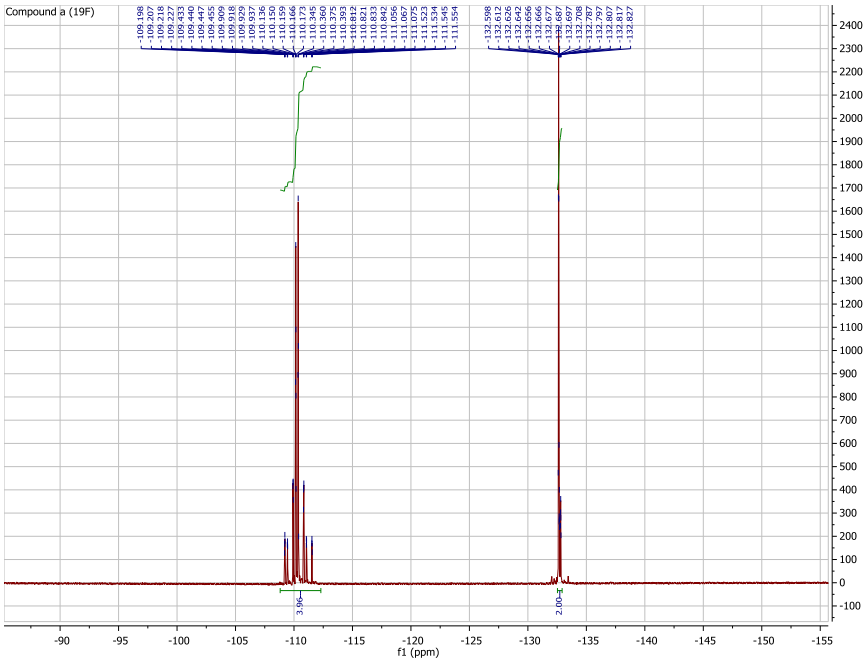

Figure S17-c. ^{19}F-NMR (367 MHz) chart of **a** in $CDCl_3$

NMR spectra of compound b

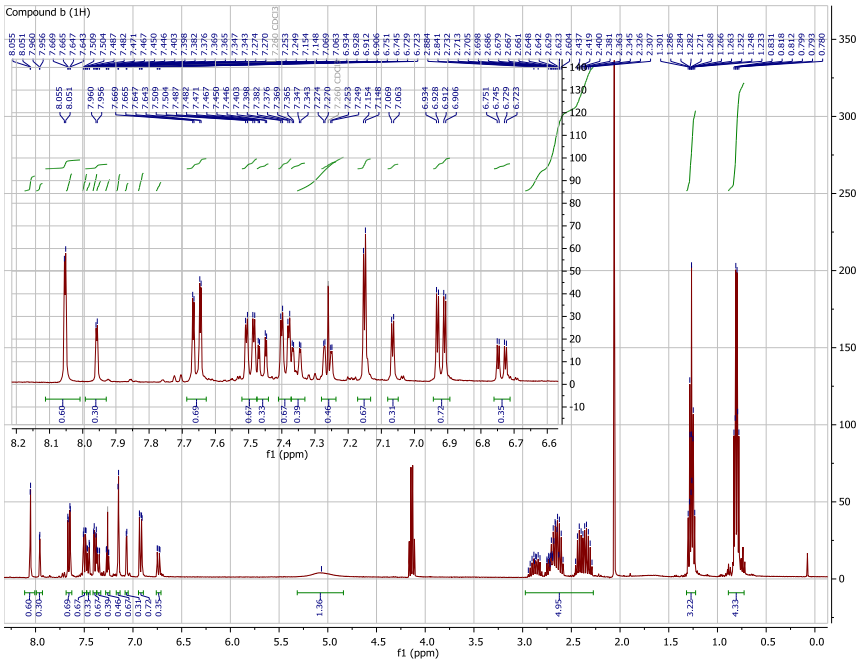

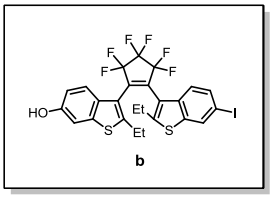

Figure S18-a. ^{1}H-NMR (400 MHz) chart of **b** in $CDCl_3$

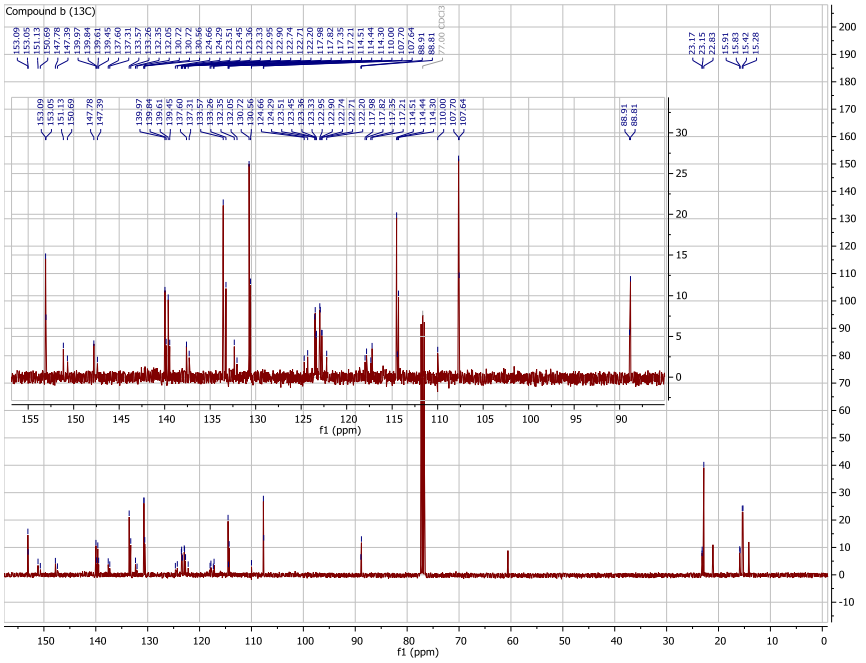

Figure S18-b. ^{13}C-NMR (101 MHz) chart of **b** in $CDCl_3$

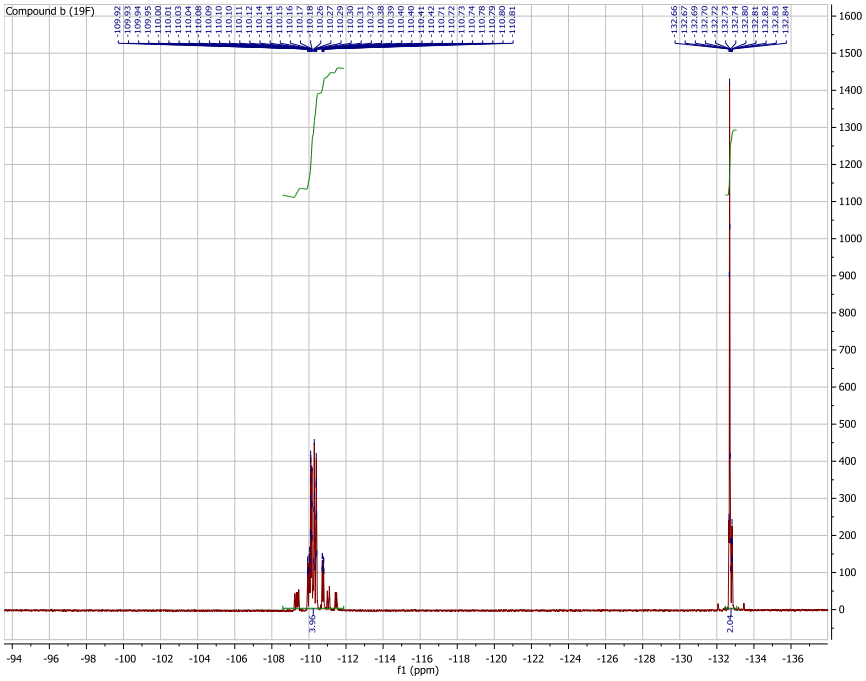

Figure S18-c. ^{19}F-NMR (367 MHz) chart of **b** in $CDCl_3$

NMR spectra of compound c

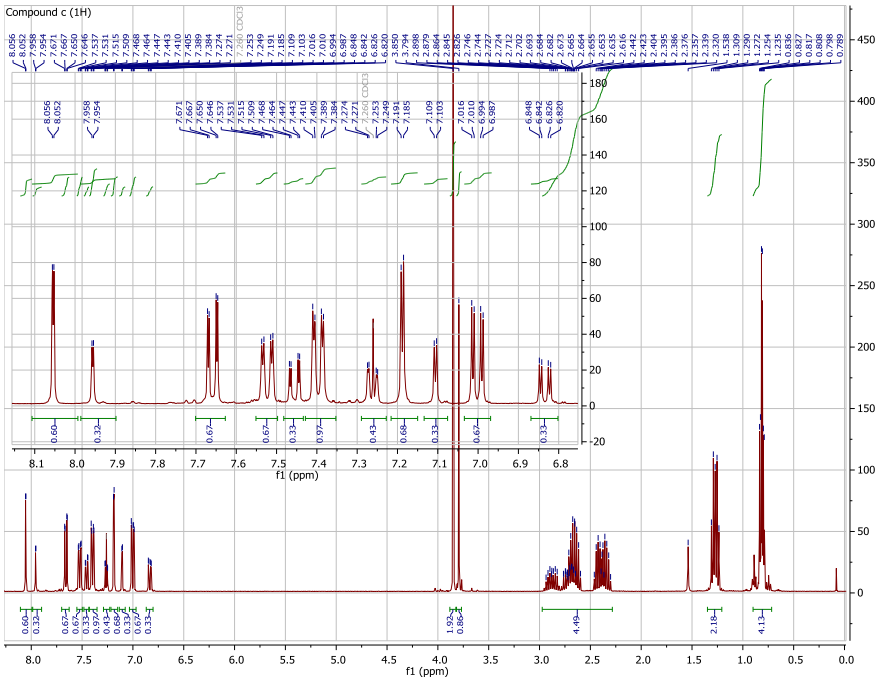

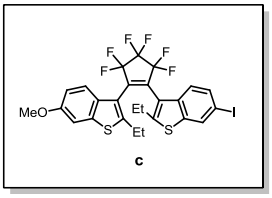

Figure S19-a. ^{1}H-NMR(400 MHz) chart of **c** in $CDCl_3$

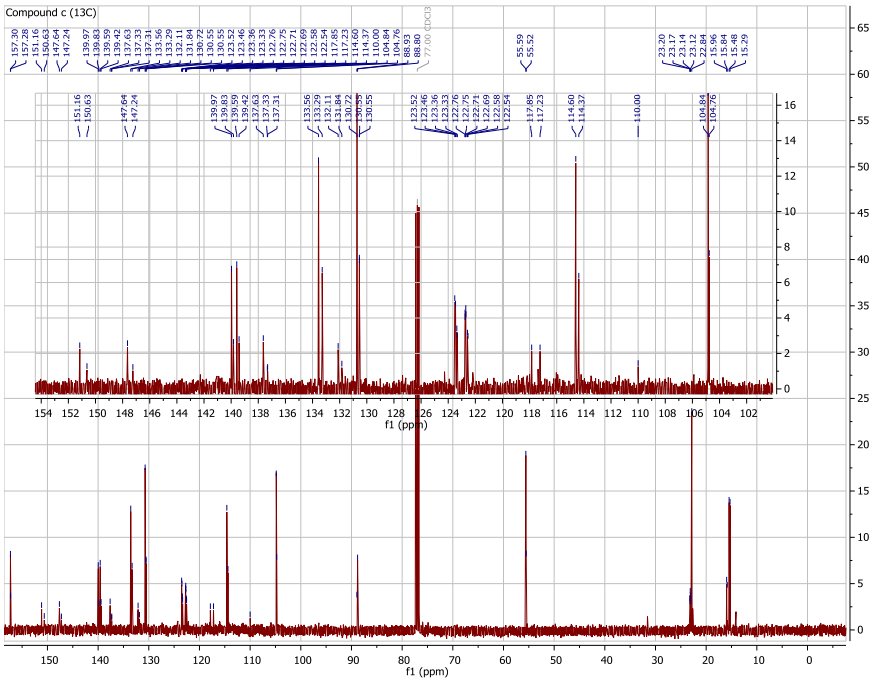

Figure S19-b. ^{13}C-NMR (101 MHz) chart of **c** in $CDCl_3$

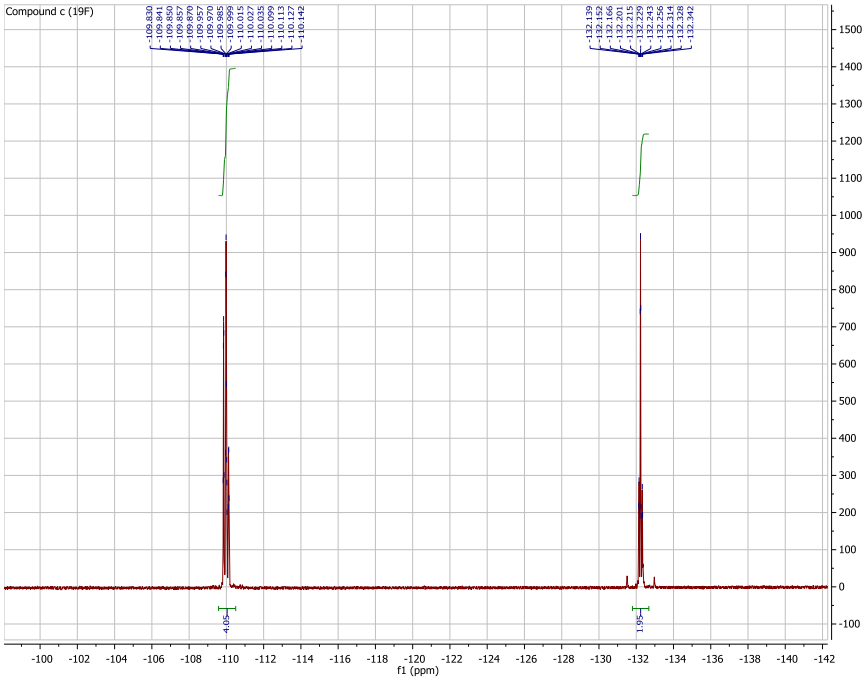

Figure S19-c. ^{19}F-NMR (367 MHz) chart of **c** in $CDCl_3$

NMR spectra of compound *d*

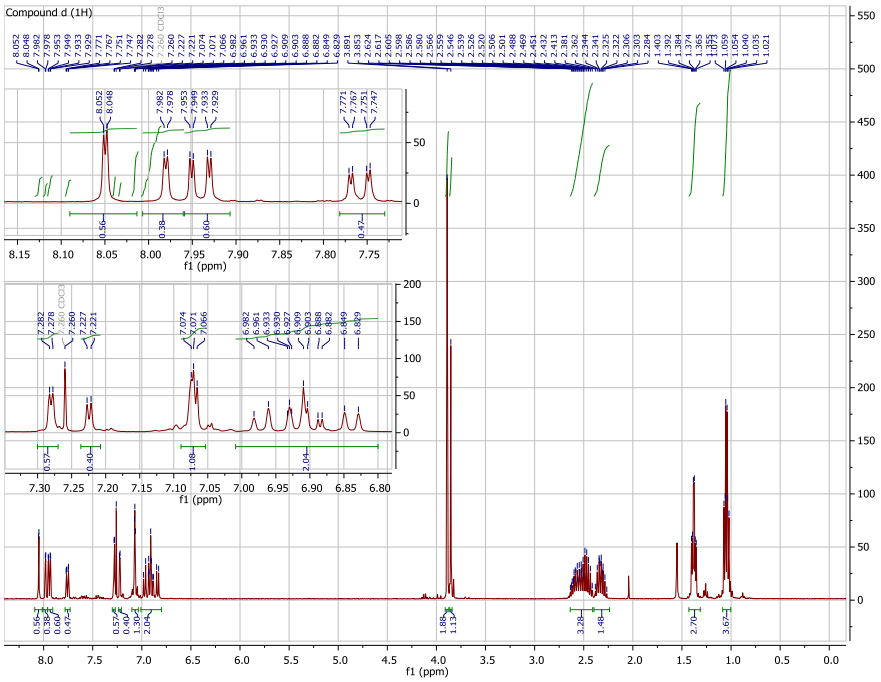

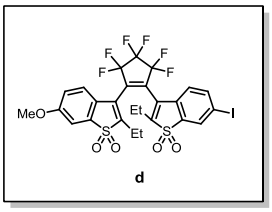

Figure S20-a. ^{1}H-NMR (400 MHz) chart of **d** in $CDCl_3$

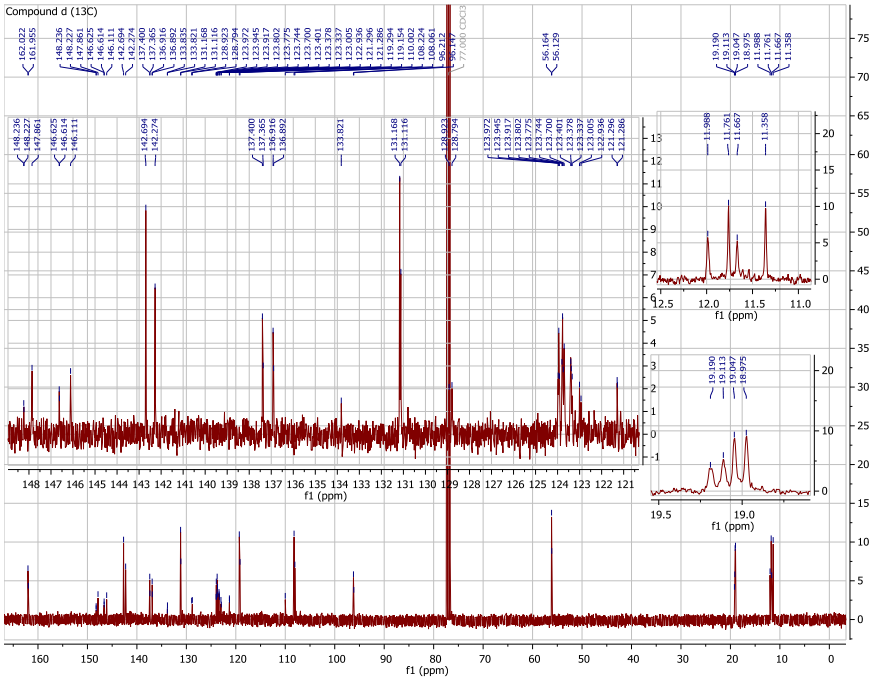

Figure S20-b. ^{13}C-NMR (101 MHz) chart of ***d*** in $CDCl_3$

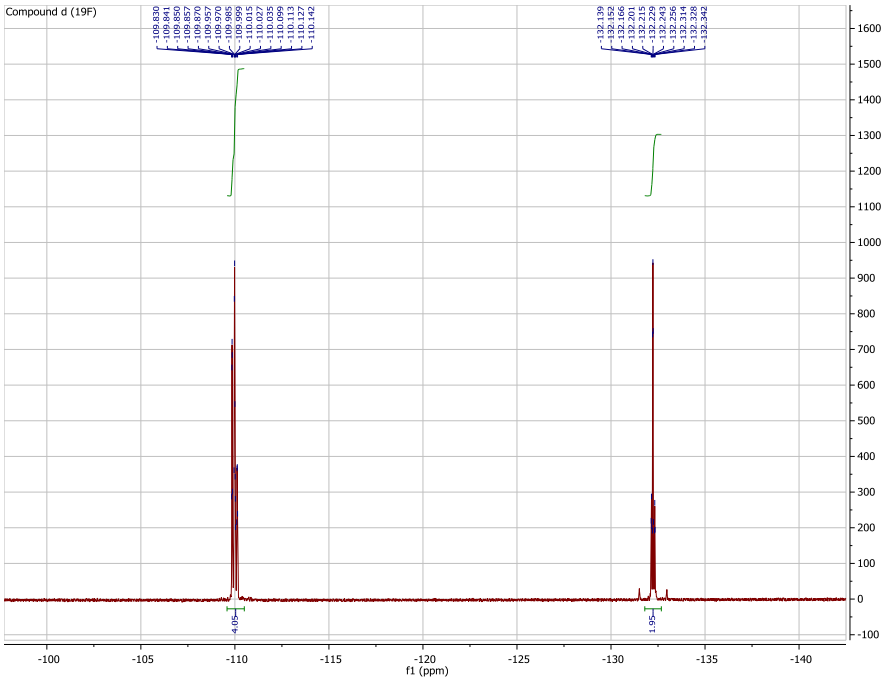

Figure S20-c. ^{19}F-NMR (367 MHz) chart of ***d*** in $CDCl_3$

NMR spectra of compound e

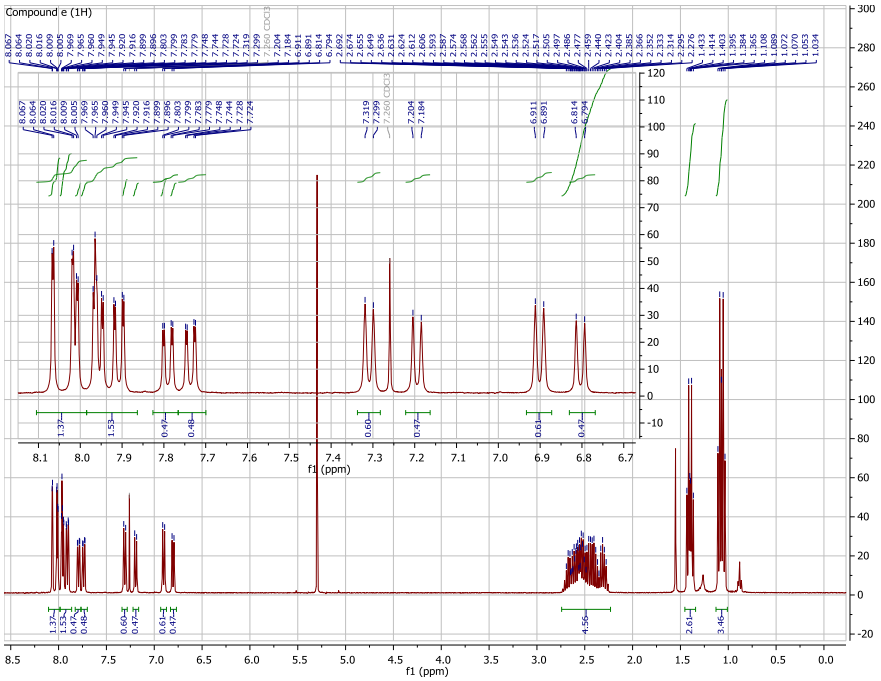

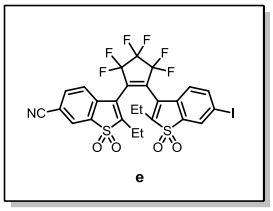

Figure S21-a. ^{1}H-NMR (400 MHz) chart of **e** in $CDCl_3$

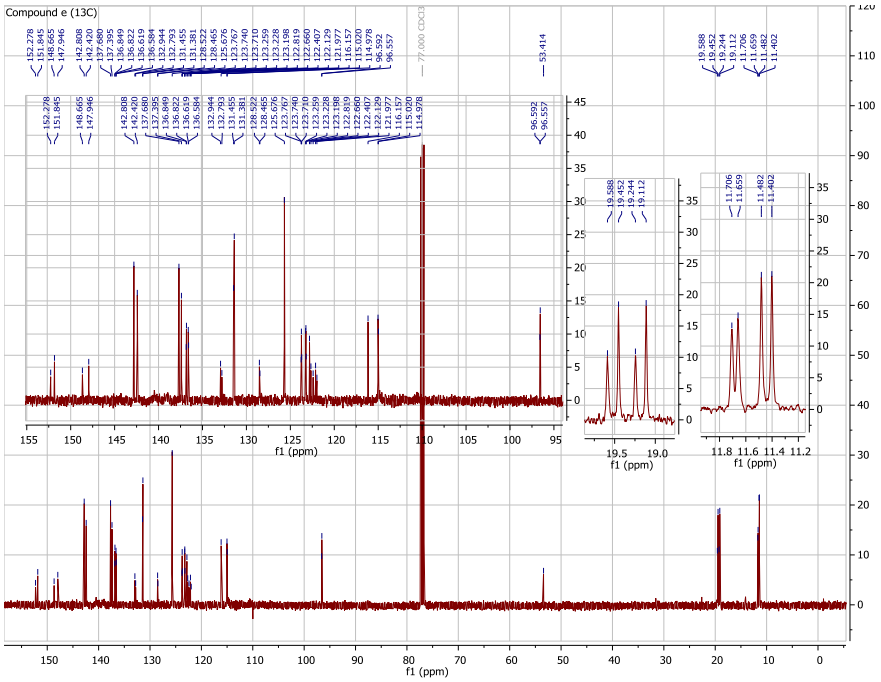

Figure S21-b. ^{13}C-NMR (101 MHz) chart of **e** in $CDCl_3$

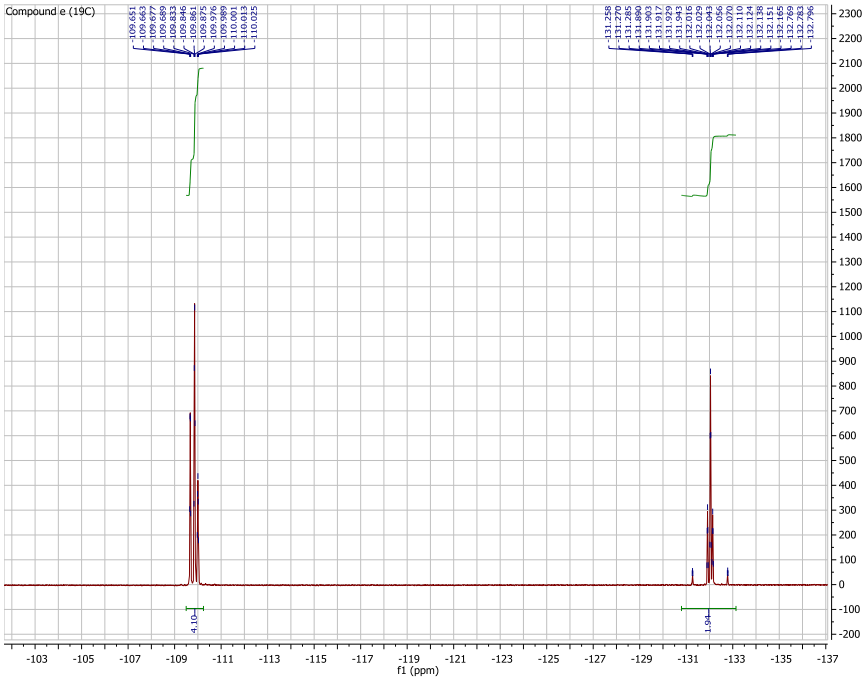

Figure S21-c. ^{19}F-NMR(367 MHz) chart of **e** in $CDCl_3$

NMR spectra of compound f

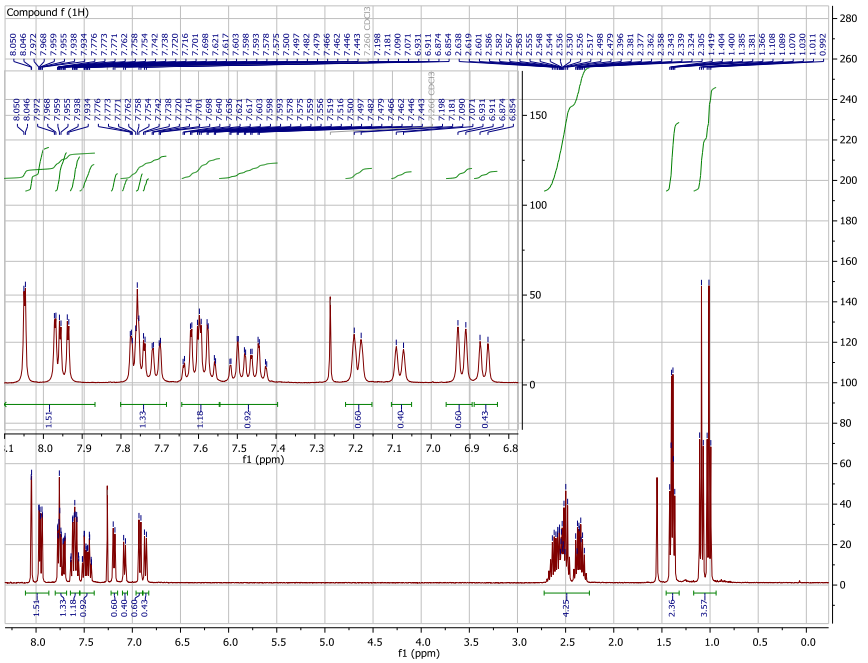

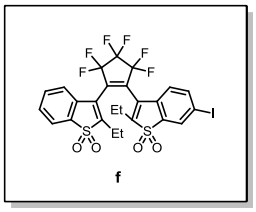

Figure S22-a. ^{1}H-NMR (400 MHz) chart of **f** in $CDCl_3$

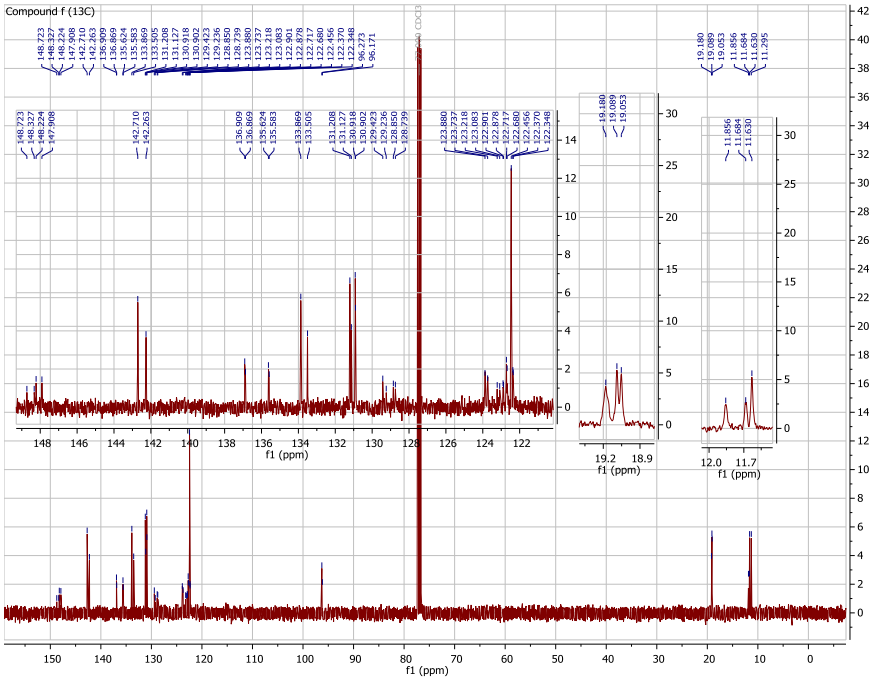

Figure S22-b. ^{13}C-NMR (101 MHz) chart of **f** in $CDCl_3$

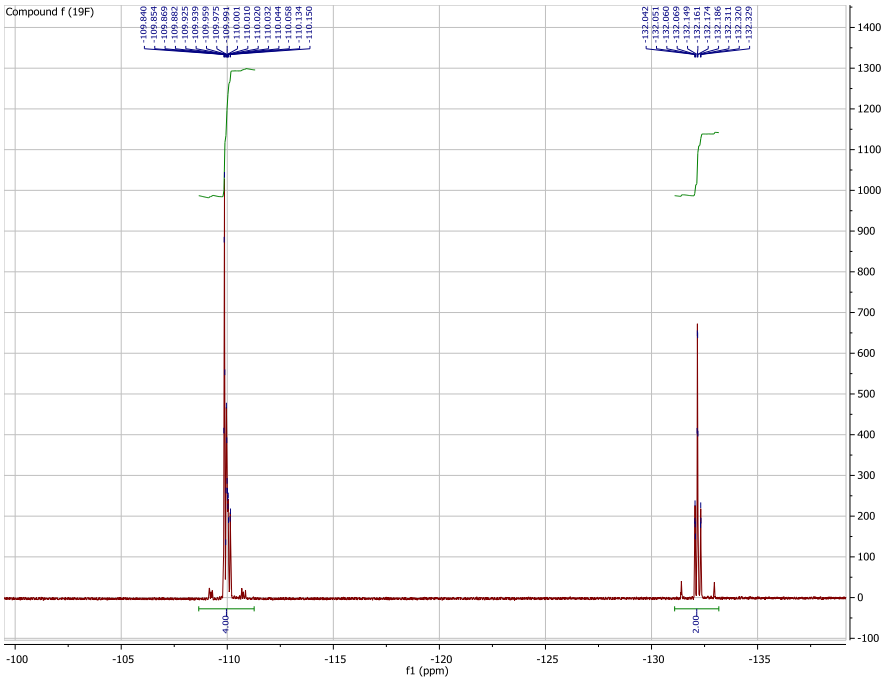

Figure S22-c. ^{19}F-NMR (367 MHz) chart of **f** in $CDCl_3$

NMR spectra of compound 1-MeO,N

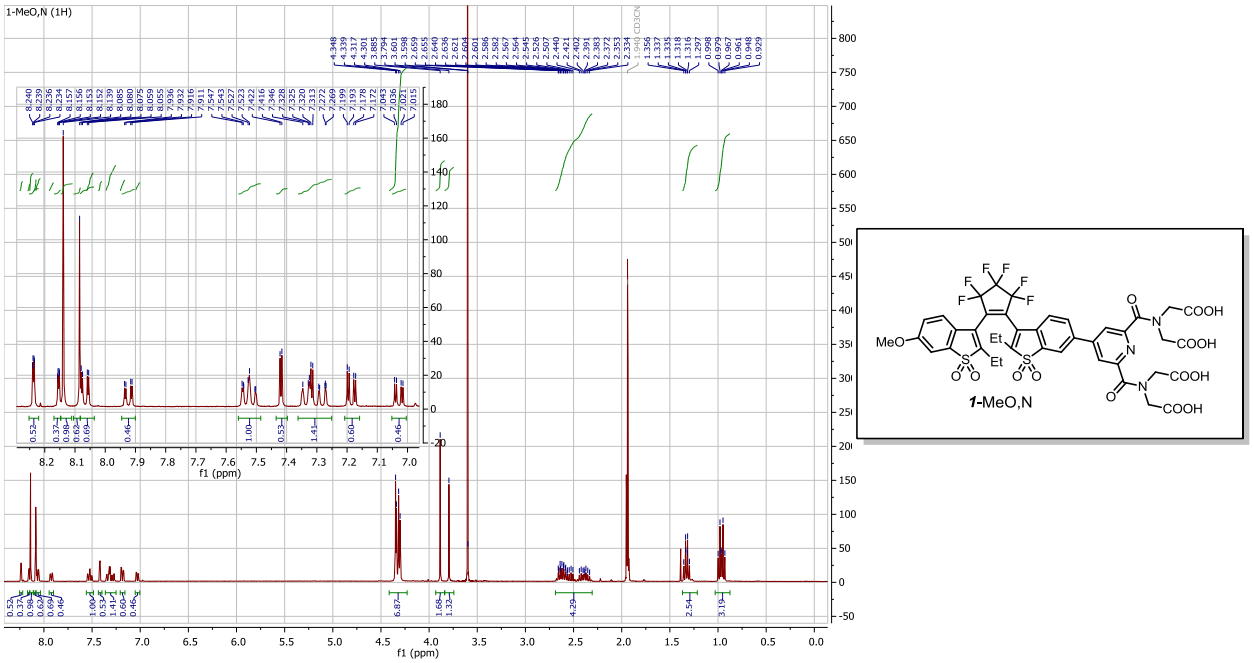

Figure S23-a. ^{1}H-NMR (400 MHz) chart of **1**-MeO,N in CD_3CN

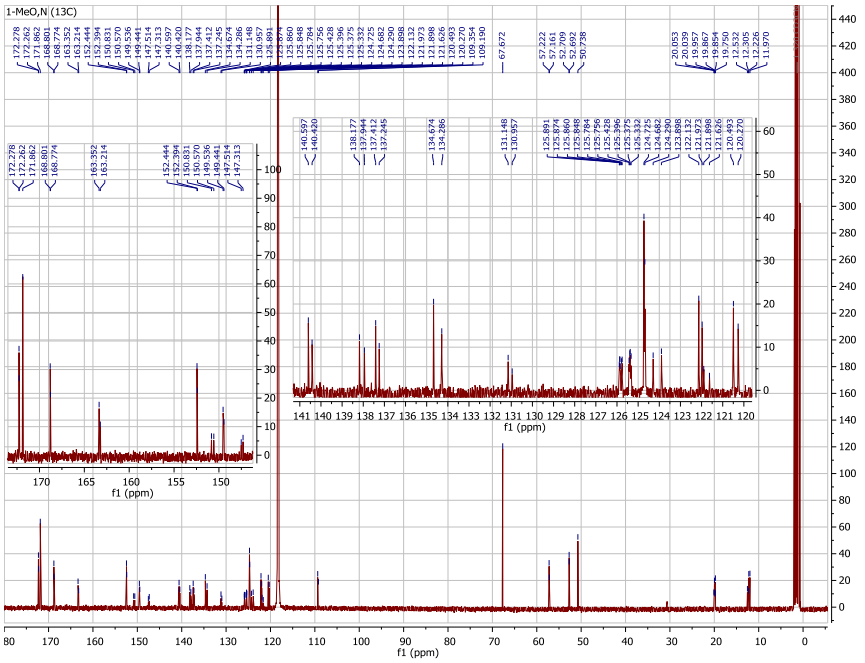

Figure S23-b. ^{13}C-NMR (101 MHz) chart of **1**-MeO,N in CD_3CN

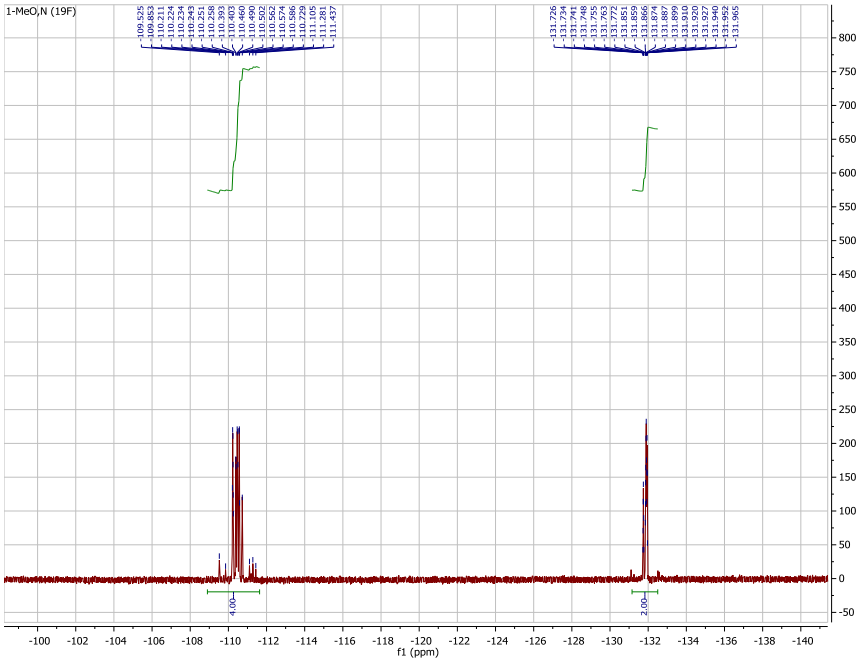

Figure S23-c. ^{19}F-NMR (367 MHz) chart of **1**-MeO,N in CD_3CN

NMR spectra of compound 1-MeO,COMe

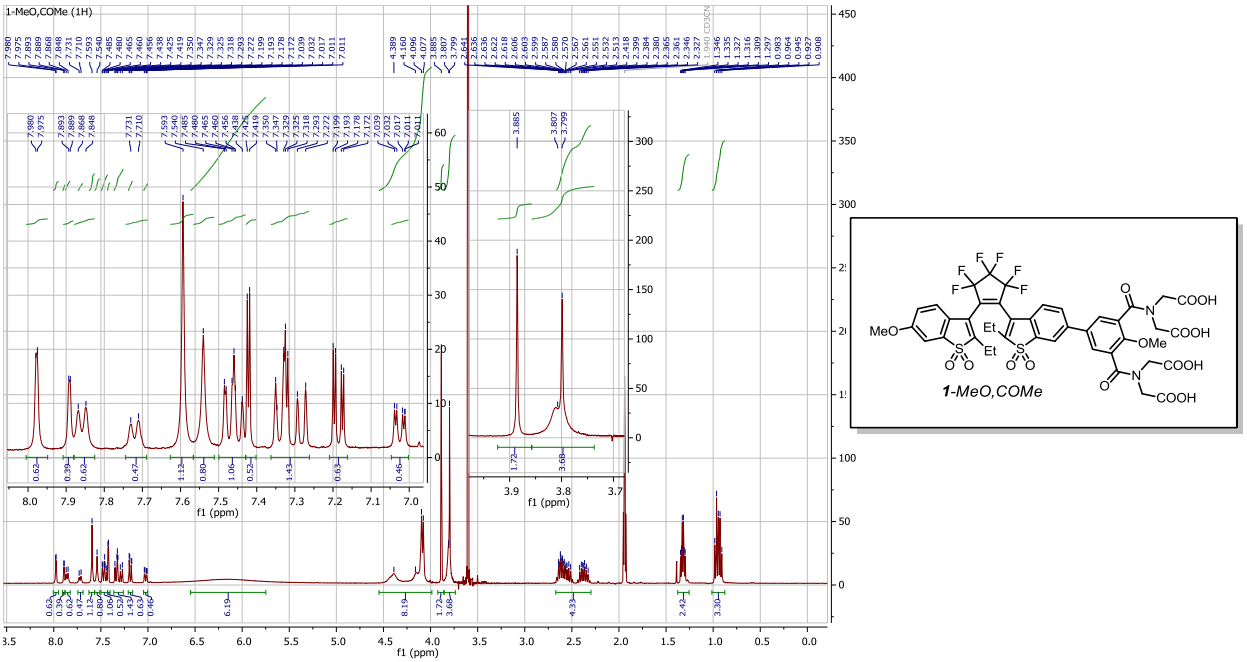

Figure S24-a. ^{1}H-NMR (400 MHz) chart of **1**-MeO,COMe in CD_3CN

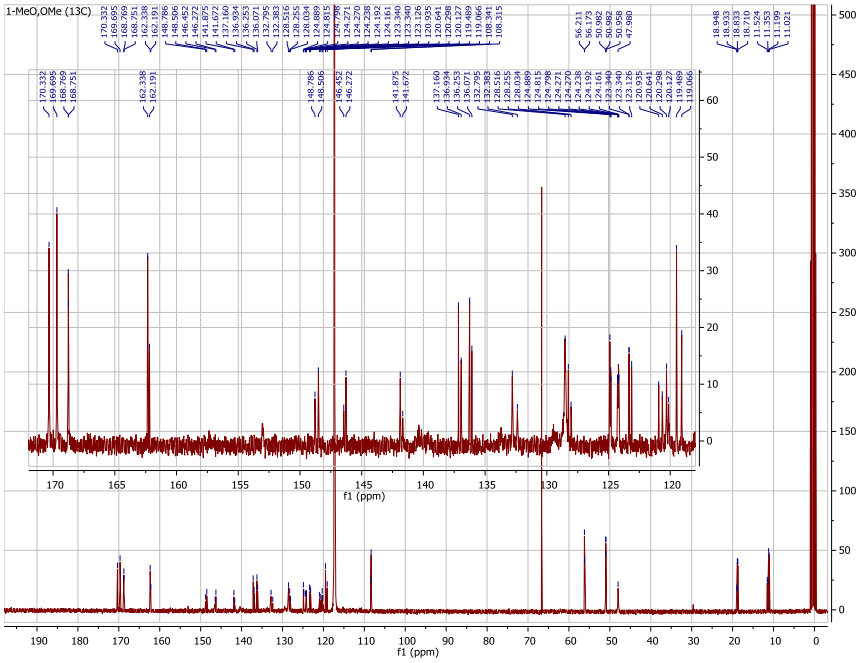

Figure S24-b. ^{13}C-NMR (101 MHz) chart of **1**-MeO,COMe in CD_3CN

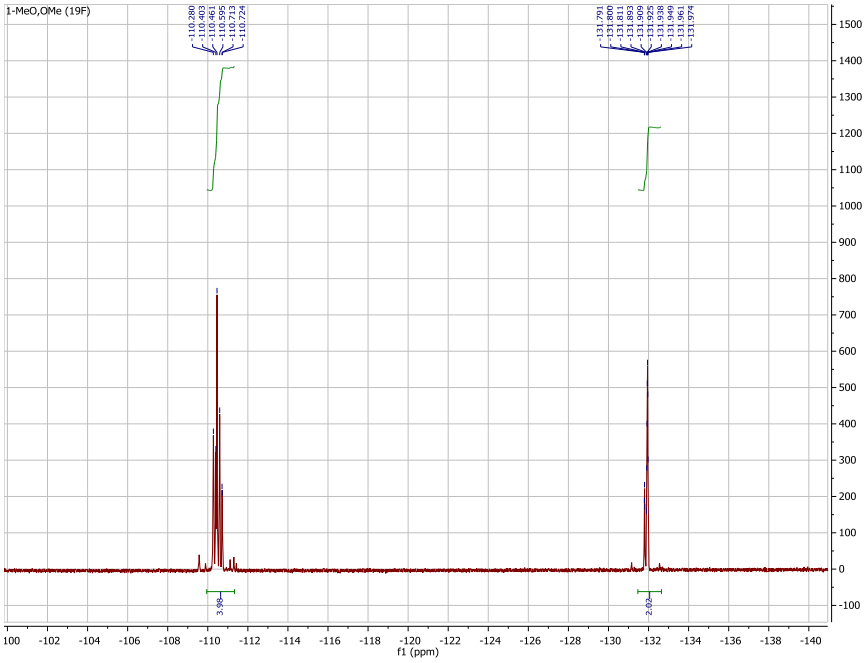

Figure S24-c. ^{19}F-NMR (367 MHz) chart of **1**-MeO,COMe in CD_3CN

NMR spectra of compound 1-CN,N

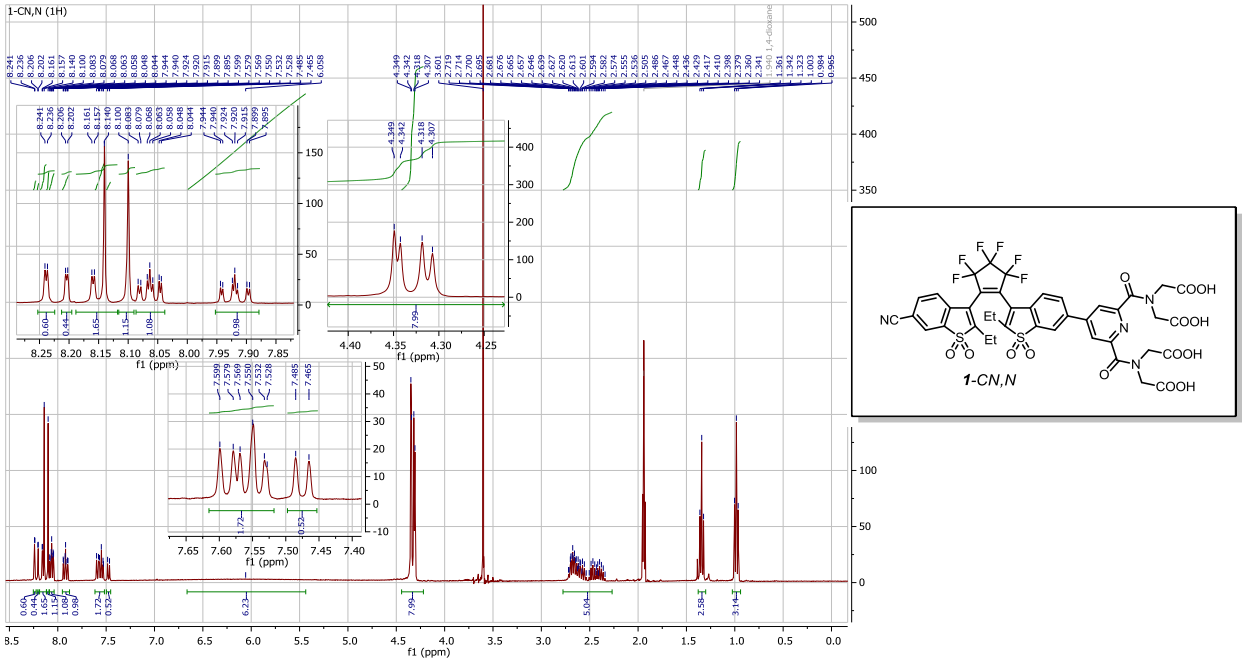

Figure S25-a. ^{1}H-NMR (400 MHz) chart of **1**-CN,N in CD_3CN

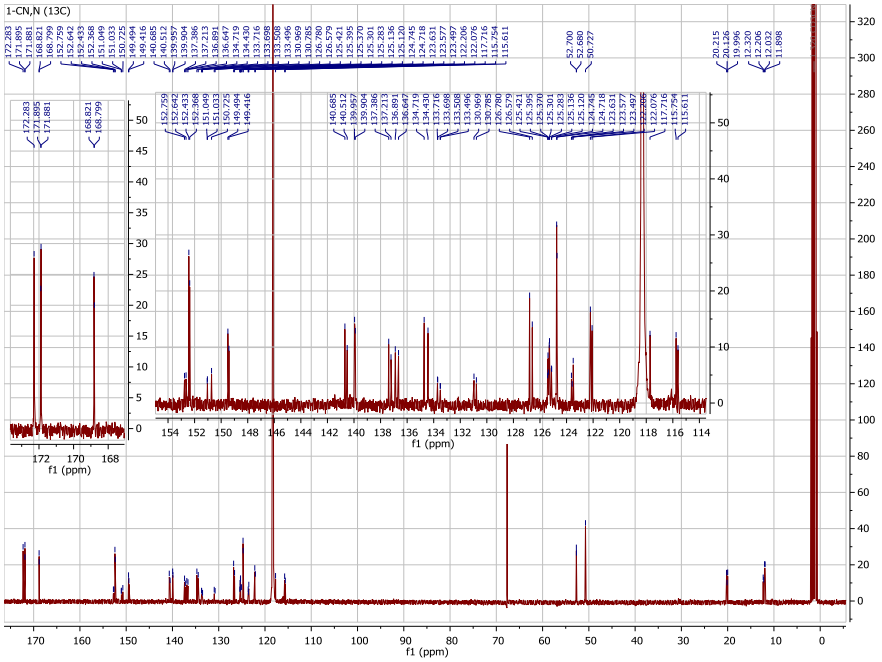

Figure S25-b. ^{13}C-NMR (101 MHz) chart of **1**-CN,N in CD_3CN

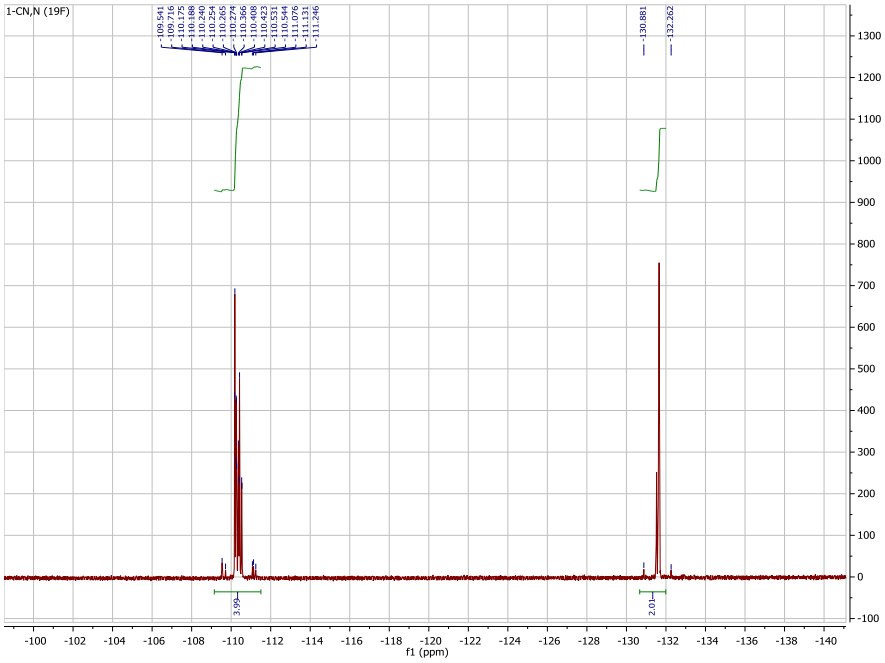

Figure S25-c. ^{19}F-NMR (367 MHz) chart of **1**-CN,N in CD_3CN

NMR spectra of compound 1-CN,COMe

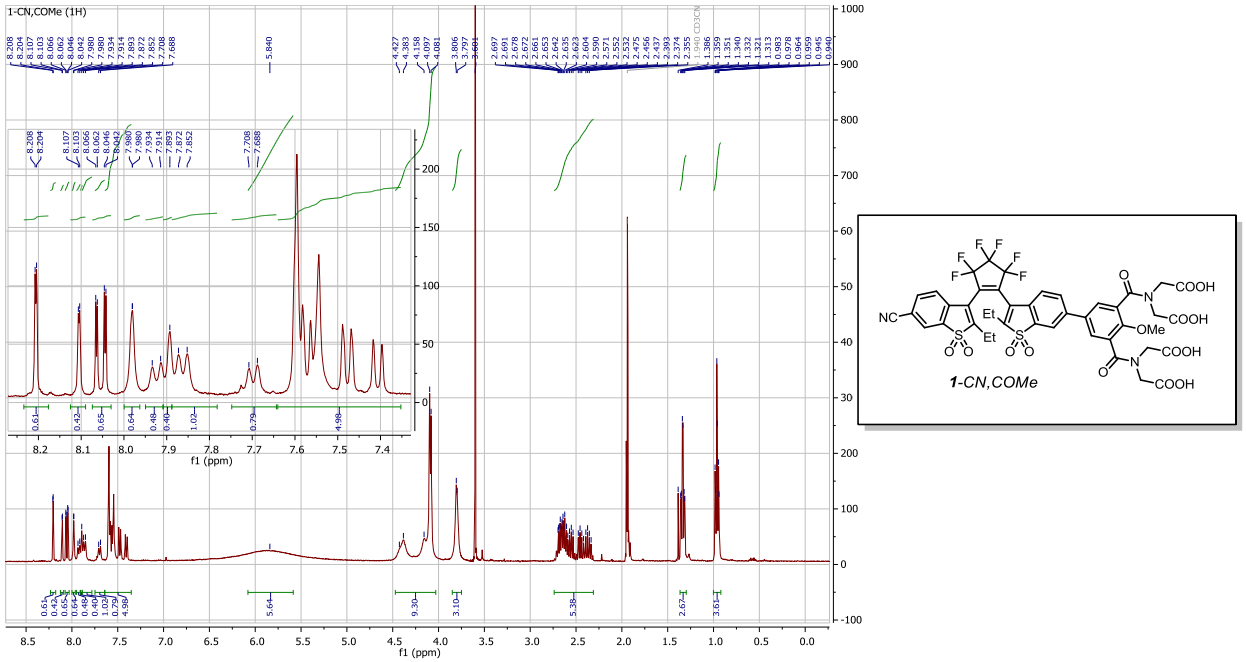

Figure S26-a. ^{1}H-NMR (400 MHz) chart of **1**-CN,COMe in CD_3CN

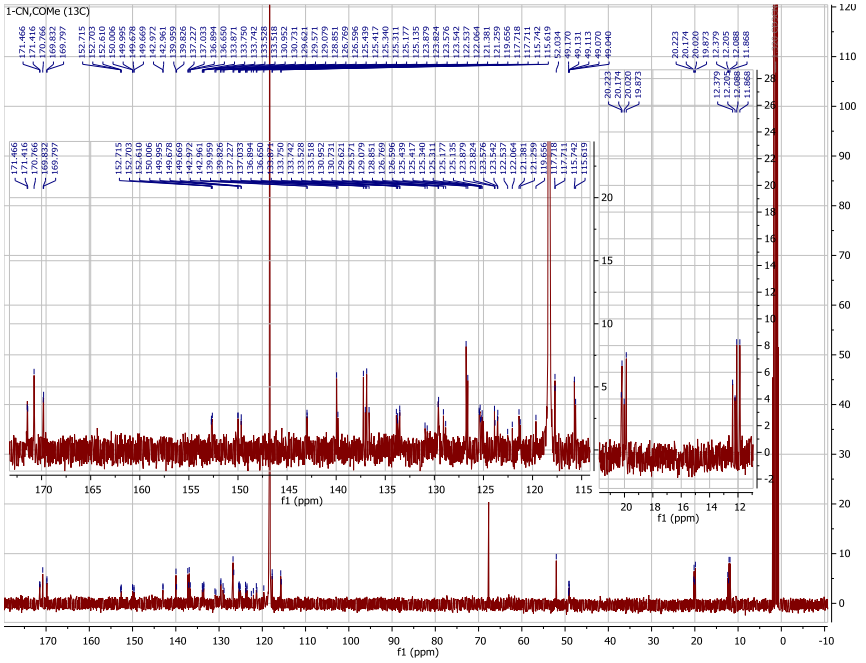

Figure S26-b. ^{13}C-NMR (101 MHz) chart of **1**-CN,COMe in CD_3CN

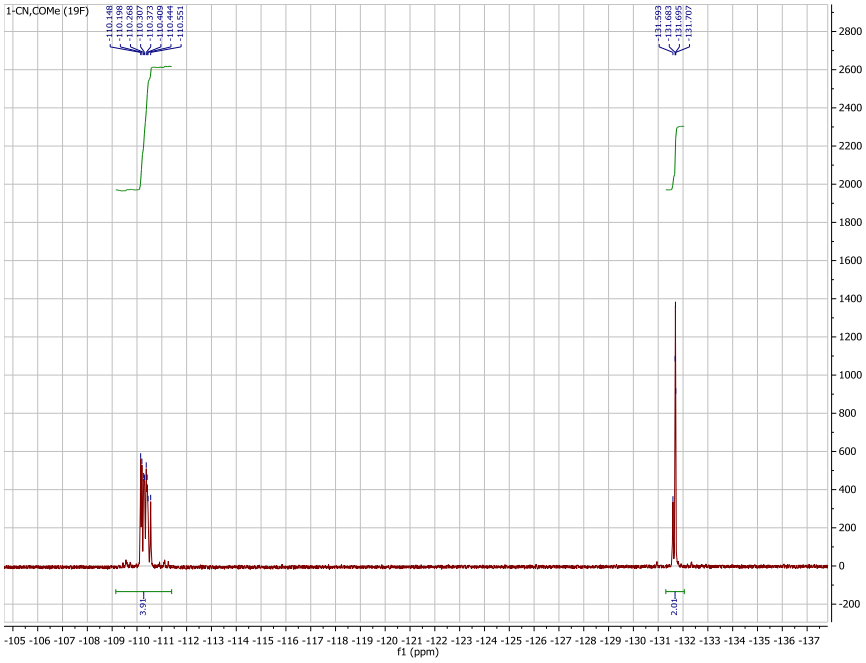

Figure S26-c. ^{19}F-NMR (367 MHz) chart of **1**-CN,COMe in CD_3CN

NMR spectra of compound *1-H,CH*

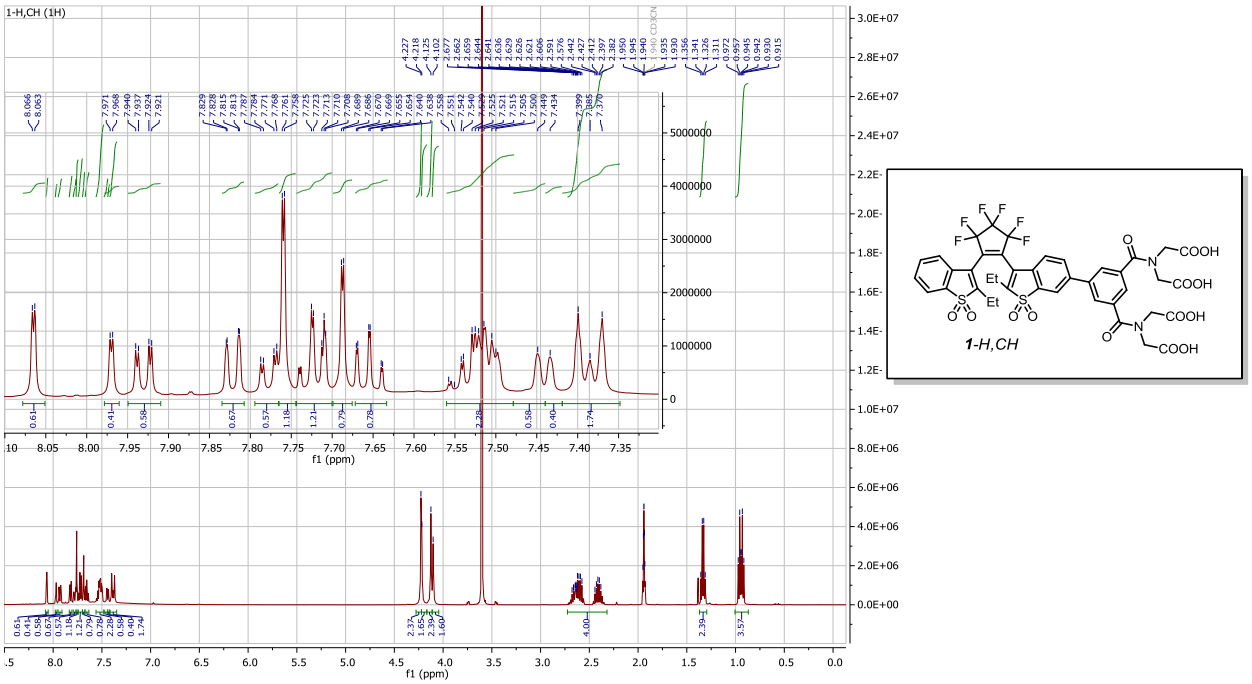

Figure S27-a. ^{1}H-NMR (500 MHz) chart of ***1-H,CH*** in CD_3CN

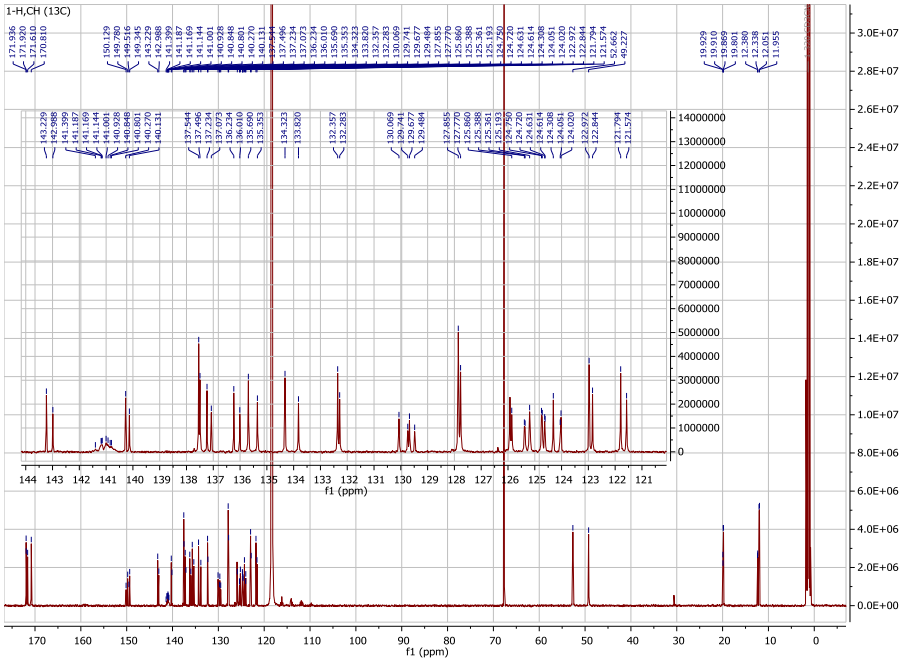

Figure S27-b. ^{13}C-NMR (126 MHz) chart of ***1-H,CH*** in CD_3CN

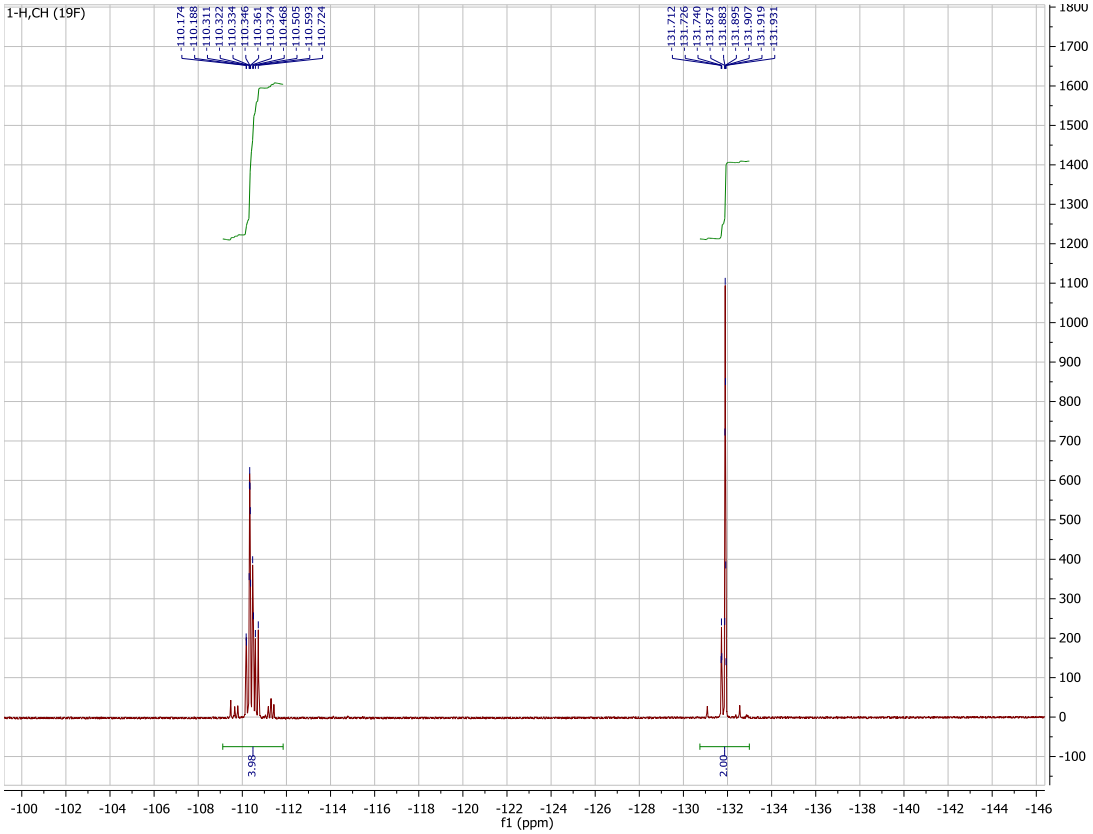

Figure S28-c. ^{19}F-NMR (367 MHz) chart of ***1****-H,CH* in CD_3CN

References

[1] H. J. Kuhn, S. E. Braslavsky, R. Schmidt, *Pure Appl. Chem.* **2004**, *76*, 2105 – 2146.

[2] G. Gauglitz, S. Hubig, *J. Photochem.* **1985**, *30*, 121.

[3] Y. Yokoyama, T. Inoue, M. Yokoyama, T. Goto, T. Iwai, N. Kera, I. Hitomi, Y. Kurita, *Bull. Chem. Soc. Jpn.* **1994**, *67*, 3297.

[4] A. Duerrbeck, S. Gorelik, J. Hobley, J. Wu, A. Hor, N. Long, *Chem. Commun.* **2015**, *51*, 8656.

[5] T. Yamaguchi, M. Irie, *J. Photochem. Photobiol. A* **2006**, *178*, 162.

[6] K. Uno, H. Niikura, M. Morimoto, Y. Ishibashi, H. Miyasaka, M. Irie, *J. Am. Chem. Soc.* **2011**, *133*, 13558.